Isoperimetric Properties of Some Genus 3 Triply Periodic Minimal Surfaces Embedded in Euclidean Space

by: Darren Matthew Garbuz, Bachelor of Science

A Thesis Submitted in Partial
Fulfillment of the Requirements
for the Master of Science Degree

Department of Mathematics and Statistics
in the Graduate School
Southern Illinois University Edwardsville
Edwardsville, Illinois

May, 2010

SOUTHERN ILLINOIS UNIVERSITY EDWARDSVILLE

GRADUATE STUDIES

WE HEREBY RECOMMEND THAT THE THESIS SUBMITTED

BY _____

ENTITLED _____

_____

_____

PRESENTED ON _____

BE ACCEPTED IN PARTIAL FULFILLMENT OF THE REQUIREMENT FOR THE

DEGREE OF _____

WITH A MAJOR IN _____

Thesis Advisory Committee:

_____
Chairperson

_____

_____

_____

_____

We certify that, in this thesis, all research involving human subjects complies with the Policies and Procedures for Research Involving Human Subjects, Southern Illinois University Edwardsville; Edwardsville, Illinois.

For theses involving animals or biohazardous material, including recombinant DNA, we certify that the research complies with the applicable policies and procedures established by the Animal Care Committee on the University Committee Biosafety, respectively, of Southern Illinois University Edwardsville; Edwardsville, Illinois.

TABLE OF CONTENTS

LIST OF FIGURES

CHAPTER 1

INTRODUCTION

The classical isoperimetric problem asks, of all closed curves in the plane ($\mathbb{R}^2$) enclosing a constant area, which curves minimize the perimeter? The solution to this problem arises from what is called the isoperimetric inequality. Let A be the area of the enclosed region and L be the length of the curve. Then the isoperimetric inequality is $4\pi A \leq L^2$. Equality holds if and only if the curve is a circle. We can extend different versions of this problem to three dimensional Euclidean space. One related and interesting problem asks: given a three dimensional Riemaniann manifold with a fixed volume, what surfaces split the volume of the manifold into two regions of equal volume while having least surface area. Finding solutions to this generalized problem would be a little too bold for this thesis, but we can still investigate candidate surfaces in specific situations.

A minimal surface is a surface where the average of the principal curvatures at every point (the mean curvature) is zero. We say a minimal surface M is triply periodic if it is invariant under the action of a rank 3 lattice Λ. The genus of a surface is a topologically invariant property of surfaces, that we will describe a little later in this thesis. We will show that it is impossible to have a triply periodic minimal surfaces with genus less than 3. The triply periodic minimal surfaces we are interested in are of genus 3. We only limit our investigation to genus 3 since they are the simplest examples of triply periodic minimal surfaces.

The first goal of this thesis is to show that genus three triply periodic minimal surfaces separate Euclidean three space into two regions and also separate the quotient space $\mathbb{R}^3/\Lambda$ into two regions of equal volume. The second goal of this thesis is to classify the symmetries of these surfaces using crystallographic space group notation. Finally, we are

interested in the surface area-to-volume ratios of families of theses surfaces. Motivation for studying these characteristics is that these surfaces are possible candidates to solve certain isoperimetric problems under situation.

Works of Ros (see [Ros03] and [Ros05]) have various theorems and conjectures for solutions to the isoperimetric problem in certain situations. Some of these results look for solutions of the isoperimetric problem for $\mathbb{R}^3/\Lambda$, when Λ is generated by an orthogonal set of three linearly independent vectors. In this thesis, we look at some triply periodic minimal surface with lattices generated by sets of vectors that are not orthogonal. It is generally accepted that these surface separate space; however, it is not mentioned why these surface actually do this in most literature. Thus, it was important to present a proof of this property in this thesis.

CHAPTER 2

PRELIMINARIES

2.1 Riemann Surfaces and Differential Forms

In this section, we define what a Riemann surface is and discuss differential forms on Riemann surfaces. To define a Riemann surface, we need a couple of definitions relating to complex manifolds.

Definition 2.1.0.1. *Let X be a Hausdorff space. Let $\{U_\alpha\}$ be an open covering of X such that for each U_α there is a complex valued function $f_\alpha : U_\alpha \to \mathbb{C}$ (called local coordinates) which is a homeomorphism of U_α onto an open set $f(U_\alpha) \subset \mathbb{C}$. If for any i, j such that $U_i \cap U_j \neq \emptyset$, the mapping $f_j \circ f_i^{-1}$ of the image $f_i(U_i \cap U_j)$ onto the image $f_j(U_i \cap U_j)$ is a holomorphic function with nowhere zero derivative, then X is called a (holomorphic) complex manifold.[Car63]*

An example of a complex manifold is $\hat{\mathbb{C}} := \mathbb{C} \cup \{\infty\}$. Let $U_1 := \mathbb{C}$ and $U_2 = \hat{\mathbb{C}} \backslash \{0\}$. Let $f_1 : U_1 \to \mathbb{C}$ be defined as $f_1(z) = z$. Let $f_2 : U_2 \to \mathbb{C}$ be defined as $f_2(\infty) = 0$ and $f_2(z) = 1/z$. The overlap functions f_{12} and f_{21} both take point a z and map z to its reciprocal $\frac{1}{z}$ and both map onto $\mathbb{C} \backslash \{0\}$. Each function is also holomorphic since $\frac{1}{z}$ is analytic in $\mathbb{C} \backslash \{0\}$.

Locally, a complex manifold "looks like" the complex plane. Since these manifolds have this complex structure, we can introduce the notion of a holomorphic function on a complex manifold.

Definition 2.1.0.2. *A continuous mapping $f : M \to N$ between two complex manifolds is called holomorphic if for every local coordinate $\{U_\alpha, f_\alpha\}$ on M and every local coordinate*

$\{V_\beta, g_\beta\}$ on N with $U_\alpha \cap f^{-1}(V_\beta) \neq \emptyset$, the mapping

$$g_\beta \circ f \circ f_\alpha^{-1} : f_\alpha\left(U_\alpha \cap f^{-1}(V_\beta)\right) \to g_\beta(V_\beta)$$

is a holomorphic mapping. [FK92]

We now have the tools to define a Riemann surface.

Definition 2.1.0.3. *A complex manifold X is called a Riemann surface if it is a one complex dimensional connected holomorphic manifold. [FK92]*

In our last example, we showed that $\hat{\mathbb{C}}$ is a complex manifold. Since $\hat{\mathbb{C}}$ is connected and has one-complex dimension, $\hat{\mathbb{C}}$ is a Riemann surface. Riemann surfaces will be used as domains of the minimal surfaces discussed in this thesis. A special type of Riemann surface if formed by the solution set of a two variable polynomial equation. These types of Riemann surface will be useful later on. The following proposition describes these types of Riemann surfaces.

Proposition 2.1.0.4. *Fix eight unique points $x_i \in \mathbb{C}$. The set*

$$X = \left\{(x, y) \in \hat{\mathbb{C}}^2 : y^2 = \prod_{i=1}^{8}(x - x_i)\right\}, \tag{2.1}$$

is a Riemann surface.

We must note that the point (∞, ∞) is a solution to the equation and is a point in X.

Proof. Put

$$P(x) := \prod_{i=1}^{8}(x - x_i).$$

First, we must show that X is a complex holomorphic manifold. Since X is a subset of a Hausdorff space $\hat{\mathbb{C}} \times \hat{\mathbb{C}}$, we have that X is Hausdorff (using the metric topology). We now need to build the complex manifold structure. For points (x, y_0) such that $y_0 \neq 0, \infty$

we take the open set $B_\epsilon(x) \times B_\epsilon(y_0)$. We want to find an ϵ small enough so that the projection $\pi_1(x, y_0) = x$ is a homeomorphism. Let ϵ_1 be chosen small enough so that $B_{\epsilon_1}(y_0)$ does not contain $-y$ for all $y \in B_{\epsilon_1}(y_0)$. Let ϵ_2 be chosen small enough so that $x_1, x_2, ..., x_8$ are not included in $B_{\epsilon_2}(x)$. Put $\epsilon = \min\{\epsilon_1, \epsilon_2\}$. Then π_1 is bijective in $B_\epsilon(x) \times B_\epsilon(y_0)$. Since π_1 is bicontinuous, π_1 is a homeomorphism. For points $(x, 0)$ we need different open sets. Since $P(x)$ has eight unique zeros. we can see that

$$P'(x) = \sum_{i=1}^{8} \prod_{j \neq i} (x - x_j)$$

is nonzero at these zeros of $P(x)$. The Implicit Function Theorem guarantees us small neighborhoods about these points such that the projection $\pi_2(x, y) = y$ is bijective. For the point (∞, ∞), we take the function $\pi_\infty(x, y) = \frac{1}{x}$, where $\pi_\infty(\infty, \infty) = 0$ as the local coordinate. The open set that we define the local coordinate in is

$$\{(x, y) : |x| > |x_i|, i = 1, ..., 8\}.$$

This projection is bijective. Now let U be be a set in the cover of the type containing a point (x, y) such that $y \neq 0$ and V be the type in the cover where it contains a point $(x, 0)$. If $U \cap V \neq \emptyset$, the mapping

$$\pi_2 \circ \pi_1^{-1}(x) = \sqrt{\prod_{i=1}^{8} (x - x_i)}$$

is single valued, bijective, and holomorphic. Thus, we have shown that X is a complex manifold. Now we show that X is a Riemann surface. To show that X is connected, we show that X is path connected. Let (x_1, y_1) and (x_2, y_2) be two points. We project to the y coordinate. Since $\sqrt{P(x)}$ is continuous, we can travel along this path until we arrive at y_2. When we inverse project, we will either be at (x_2, y_2) or $(-x_2, y_2)$ since the square root is a multivalued function. If the later occurs, we can make an

analytic continuation. We do this by looping once around a zero. Then, when we inverse project, we arrive at (x_2, y_2). Hence, X is path connected. Now we show that X has one complex dimension. When developing the complex manifold structure, we showed that the projections π_1 or π_2 are homeomorphisms in small enough balls around any point. Thus X is locally homeomorphic to $\mathbb{C}$. Since X is connected and locally homeomorphic to a one-dimensional complex space, X has one complex dimension. Hence X is a Riemann surface. □

We also need some definitions and theorems about differentiable forms on Riemann surfaces because they will help us prove some propositions latter on.

Definition 2.1.0.5. *Let X be a Riemann surface. We define a 1-form ω on X as an ordered assignment f and g to each local coordinate $z\,(= x + iy)$ on X such that*

$$f\,dx + g\,dy$$

satisfies the following: If z and z^* are local coordinates on X and the domain of z^* intersects non-trivially the domain of z, and if ω assigns the functions f^*, g^* to z^*, then

$$\begin{pmatrix} f^*(z^*) \\ g^*(z^*) \end{pmatrix} = \begin{pmatrix} \frac{\partial x}{\partial x^*} & \frac{\partial x}{\partial y^*} \\ \frac{\partial y}{\partial x^*} & \frac{\partial y}{\partial y^*} \end{pmatrix} \begin{pmatrix} f(z(z^*)) \\ g(z(z^*)) \end{pmatrix}$$

on the overlap of the domains of z and z^*. [FK92]

Definition 2.1.0.6. *Let X be a Riemann surface and ω be a 1-form on X. Let $c : [0,1] \to X$ with $c(t) = x(t) + iy(t)$ be a piecewise differentiable curve in a single coordinate disc $z = x + iy$. If ω is given by the previous definition, then*

$$\int_c \omega = \int_0^1 \left(f(x(t), y(t)) \frac{dx}{dt} + g(x(t), y(t)) \frac{dy}{dt} \right) dt$$

[FK92]

If we need to integrate over multiple coordinate patches, we can break up the curve. This is okay since there is an agreement on overlaps that was given in Definition 2.1.0.5.

Definition 2.1.0.7. *Let ω be a 1-form on a Riemann surface X. If the coefficient functions are C^1, we call ω a C^1 form. We define the operator d as*

$$df = \frac{\partial f}{\partial x}\,dx + \frac{\partial f}{\partial y}\,dy$$

for C^1 functions f and

$$\begin{aligned} d\omega &= d\left(f\,dx\right) + d\left(g\,dy\right) \\ &= \left(\frac{\partial g}{\partial x} - \frac{\partial f}{\partial y}\right) dx\,dy \end{aligned}$$

[FK92]

We now define what it means for a one form to be holomorphic.

Definition 2.1.0.8. *A 1-form ω on a Riemann surface X is called holomorphic provided in each coordinate patch, $\omega = df$ with f holomorphic. [FK92]*

For certain theorems to hold, we will require our Riemann surfaces to be hyperelliptic. To define a hyperelliptic surface, we need to first know what a covering manifold is.

Definition 2.1.0.9. *A Riemann surface X^* is said to be a branched covering manifold of a manifold X provided there is a continuous surjective map (called a covering map) $f : X^* \to X$ with the following properties:*

- *For each $p \in X^*$, there exist a local coordinate z^* on X^* such that $z^*\left(p^*\right) = 0$.*
- *There exist a local coordinate z on X such that $z(f(p)) = 0$*
- *There exist an integer $n > 0$ such that f is given by $z = z^{*n}$ in terms of local coordinates.*

This number n is denoted $b_f(P)$. If $n > 1$, we call p a branch point of order $n-1$ or a ramification point of order n. The covering manifold and the map f are called ramified if $b_f(p) > 1$ for some p. If $n = 1$ for all points in X^*, then the cover is called smooth or unramified. [FK92]

Definition 2.1.0.10. *A Riemann surface X is called hyperelliptic if X is a two sheeted branched cover of a sphere.[Mee90]*

The Riemann surface

$$X = \left\{ (x, y) \in \hat{\mathbb{C}}^2 : y^2 = \prod_{i=1}^{8} (x - x_i), \ x_i \in \mathbb{C} \right\} \tag{2.2}$$

is a hyperelliptic Riemann surface and all hyperelliptic Riemann surfaces can be written in the form

$$X = \left\{ (x, y) \in \hat{\mathbb{C}}^2 : y^2 = \prod_{i=1}^{2g+2} (x - x_i), \ x_i \in \mathbb{C} \right\}, \tag{2.3}$$

for some nonnegative integer g.[FK92].

One important property of Riemann surfaces and surfaces in general, is a topological property called the genus. Informally, the genus of a surfaces is the "number of holes" in the surface. The genus of a sphere would be 0. The genus of an $n-$torus is n. We need a way to identify the genus of (orientable) Riemann surfaces.

Theorem 2.1.0.11. *Any compact Riemann surface is either homeomorphic to a sphere, to a connected sum of tori, or to a connected sum of projective planes. [Mas91]*

With this theorem, we can associate a genus to a Riemann surface. If a Riemann surface is homeomorphic to a genus g surface, then the Riemann surface has genus g. The Riemann surfaces we will be using are of genus 3 so that we can to satisfy some theorems regrading automorphisms on these surfaces. The following theorem limits the order of automorphisms on genus 3 hyperelliptic Riemann surfaces.

Lemma 2.1.0.12. *Let X be a hyperelliptic Riemann surface of genus 3 and let $T : X \to X$ be an automorphism. If $X/\langle T \rangle$ has genus 1, then T has order 2,3, or 4. [Wey06]*

The next theorem places restrictions on the number of points left fixed by a (non-trivial) automorphism and introduces a special automorphism called the hyperelliptic involution.

Lemma 2.1.0.13. *Let X be a hyperelliptic Riemann surface of genus 3 covered by $f : X \to S^2$.*

1. *The function f has 8 branch points $B = \{p_1, p_2, ..., p_8\}$. These points are called the Weierstrass points.*

2. *There exists an automorphism $\iota : X \to X$ such that $\iota p_i = p_i$ and that interchanges two sheets. The function ι is called the hyperelliptic involution. Furthermore, ι is the unique involution that fixes the Weierstrass points.*

3. *For every automorphism T on X, $T(B) = B$.*

4. *If $T \neq \iota$, then T fixes no more than four points. [Wey06]*

2.2 Minimal Surfaces

In this section we discuss some basics of minimal surfaces.

Definition 2.2.0.14. *A surface X in $\mathbb{R}^3$ is called minimal if X has mean curvature zero.*

A classical example of a minimal surface is a catenoid. The catenoid is a surface of revolution formed by rotating a catenary curve.

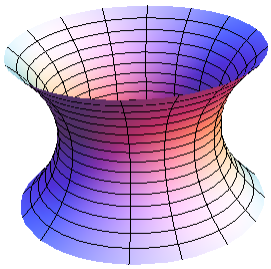

Figure 2.1: The Catenoid

One property of a surface having zero mean curvature is shown in the following theorem.

Lemma 2.2.0.15. *If X is a minimal surface, then the Gaussian curvature of X is non-positive.*

Proof. Let κ_1 and κ_2 be the maximum and minimum principal curvatures at a point on X. Since X is minimal, $\frac{\kappa_1+\kappa_2}{2} = 0$. Thus, $\kappa_1 = -\kappa_2$. This implies $\kappa_1\kappa_2 \leq 0$. □

There are many ways to parameterize a minimal surface. Since this is the case, we would like a canonical expression in which we can write all minimal surfaces. We would also like these surfaces to be parametrized in a way where we can conveniently do calculation and create pictures. We will use what is called the Weierstrass representation.

Theorem 2.2.0.16. *Let X be a Riemann surface and let $\omega_1, \omega_2, \omega_3$, be three holomorphic 1-forms with $\sum \omega_j^2 \equiv 0$ and $\sum |\omega_j|^2 \neq 0$. After a translation, any minimal surface $f : X \to \mathbb{R}^3$ can be represented by*

$$f(z) = \mathrm{Re} \int_{z_0}^{z} (\omega_1, \omega_2, \omega_3),$$

where $\omega_1 = (1 - g^2)\, dh, \omega_2 = (1 + g^2)\, i\, dh, \omega_3 = 2g\, dh$, where dh is a one-form, and g is the stereographic projection of the Gauss map onto $\hat{\mathbb{C}}$. [Mee90]

The form dh is called the height differential. We can now define any minimal surface with the Weierstrass data (X, g, dh). The catenoid discussed above has the the Weierstrass data $g(z) = z$ and $dh = dz$ [Web04]. We can construct new minimal surfaces with the Weierstrass data $(X, g, e^{i\theta}dh)$ since $\sum e^{2i\theta}\omega_j^2 \equiv 0$ and $\sum |\omega_j|^2 \neq 0$ still holds. The family of surfaces M_θ $(0 \leq \theta \leq \frac{\pi}{2})$ is called the associate family of M_θ. The helicoid is a minimal surface that is a member of the catenoid's associate family. The helicoid has the same data except for the height differential, which is multiplied by $e^{i\pi/2}$. Now we need a way to explicitly write down the Gauss maps of the surfaces. We present a way to do so in the following section.

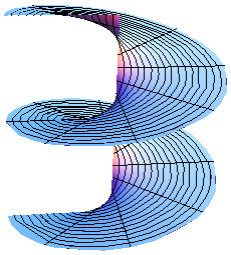

Figure 2.2: The Helicoid

2.3 Theta Functions

Let Γ be a lattice in $\mathbb{C}$ generated by 1 and τ, where $\mathrm{Re}(\tau) > 0$ and$\mathrm{Im}(\tau) > 0$. In this section, we use what are called theta functions to build Gauss maps. Our goal is to find an explicit functions on $\mathbb{C}/\Gamma$ that are doubly-periodic and meromorphic so that we can define a theta function. The following proposition addresses why we can not have doubly-periodic nonconstant holomorphic functions.

Proposition 2.3.0.17. *Let $f : \mathbb{C} \to \mathbb{C}$ be a holomorphic function. If there exists $a, b \in \mathbb{R}$ such that $f(z+a) = f(z)$ and $f(z+bi) = f(z)$, then f is constant.*

Proof. Let $A = \{z \in \mathbb{C} : 0 \leq Re(z) \leq a, 0 \leq Im(z) \leq b\}$. Since f is continuous on a compact set, there exists a $w \in A$ such that $|w| \geq |f(z)|$ for all $z \in A$. By Liouville's Theorem, f is constant in A. Since f is doubly-periodic, f is constant on all of $\mathbb{C}$. □

This shows that we cannot have a non-constant doubly-periodic holomorphic function. Since we will be using these functions for Gauss maps, we would like to allow finitely many poles. Thus, it is reasonable to use meromorphic functions instead. Let $f : \mathbb{C} \to \hat{\mathbb{C}}$ have the properties

$$f(z+1) = f(z) \tag{2.4}$$

and

$$f(z+\tau) = e^{az+b} f(z), \tag{2.5}$$

where $a, b \in \mathbb{C}$. We then have ourselves an almost doubly periodic meromorphic function.

Using Equations (2.4) and (2.5), we have

$$\begin{aligned} f(z+1+\tau) &= f(z+\tau) \\ &= e^{az+b} f(z) \end{aligned} \tag{2.6}$$

and

$$\begin{aligned} f(z+1+\tau) &= e^{a(z+1)+b} f(z+1) \\ &= e^{a} e^{az+b} f(z). \end{aligned} \tag{2.7}$$

From Equations (2.6) and (2.7), $e^a = 1$. This shows that $a = 2\pi i n$ for some $n \in \mathbb{Z}$. Since the function is periodic in the real direction, we can write the Fourier series

$$f(z) = \sum_{j \in \mathbb{Z}} c_j e^{2\pi i j z}. \tag{2.8}$$

The Fourier series representation of f and Equation (2.5) gives us

$$f(z+\tau) = \sum_{j \in \mathbb{Z}} c_j e^{2\pi i j z} e^{2\pi i j \tau}. \tag{2.9}$$

We also have that

$$\begin{aligned} f(z+\tau) &= e^{2\pi i n z} e^{b} f(z) \\ &= e^{2\pi i n z} e^{b} \sum_{j \in \mathbb{Z}} c_j e^{2\pi i j z} \\ &= e^{b} \sum_{j \in \mathbb{Z}} c_j e^{2\pi i (j+n) z} \\ &= e^{b} \sum_{j \in \mathbb{Z}} c_{j-n} e^{2\pi i j z}. \end{aligned} \tag{2.10}$$

We are then left with

$$c_j e^{2\pi i j \tau} = e^{b} c_{j-n}. \tag{2.11}$$

For $n = 0$, $f(z) = e^{2\pi iz}$. This is a function that satisfies the our requirements, but not that interesting of a function. If $n > 0$ the coefficients grow without bound. This convergence problem can be avoided for negative n. For simplicity, take $n = -1$ and put $c_0 = 1$. Then

$$c_j = e^{-jb-\pi ij\tau+\pi ij^2\tau}. \tag{2.12}$$

Once again for simplicity, set $b = -\pi i\tau$. We need to show that

$$\sum_{j\in\mathbb{Z}} e^{\pi ij^2\tau+2\pi ijz} \tag{2.13}$$

is finite. For the terms in the series where $j \geq 0$ we have

$$\begin{aligned}
\lim_j \left|\frac{z_{j+1}}{z_j}\right| &= \lim_j \left|\frac{e^{\pi i(j+1)^2\tau+2\pi i(j+1)z}}{e^{\pi ij^2\tau+2\pi ijz}}\right| \\
&= \lim_j \left|e^{\pi i(2j+1)\tau+2\pi iz}\right| \\
&= \lim_j \left|e^{-2\pi iz}\right| \left|e^{2\pi i\mathrm{Re}(\tau)(2j+1)}\right| \left|e^{-2\pi\mathrm{Im}(\tau)(2j+1)}\right| \\
&= \left|e^{-2\pi iz}\right| \lim_j | \left|e^{-2\pi\mathrm{Im}(\tau)(2j+1)}\right| \\
&= 0.
\end{aligned} \tag{2.14}$$

For the terms in the series where $j < 0$, we can use a similar argument to show convergence. Since the series converges for the negative and positive j, the series converges. We can now safely define

$$\theta_{0,0}(z,\tau) := f(z) = \sum_{j\in\mathbb{Z}} e^{\pi ij^2\tau+2\pi ijz}. \tag{2.15}$$

We make some alteration to this function and define

$$\theta(z,\tau) := e^{\pi i\frac{\tau}{4}+\pi i\left(z+\frac{1}{2}\right)}\theta_{0,0}\left(z+\frac{1}{2}+\frac{\tau}{2},\tau\right). \tag{2.16}$$

This function in (2.16) is called a theta function. The properties given by the following lemma motivates the changes we made in Equation (2.15) to get Equation (2.16).

Lemma 2.3.0.18. *The function $\theta(z,t)$ has the following properties:*

1. $\theta(z+1,\tau) = -\theta(z,\tau)$
2. $\theta(z+\tau,\tau) = -e^{-2\pi i\left(z+\frac{\tau}{2}\right)}\theta(z,\tau)$
3. $\theta(0,\tau) = 0$
4. $\theta(z,\tau)$ *has no further zeros in* $[0,1)\times[0,\tau)$

[Wey06]

The next lemma finishes our search for a double-periodic meromorphic function.

Lemma 2.3.0.19. *Consider the points $\{p_j\}_{j=1}^n$ and $\{q_j\}_{j=1}^n$ in $[0,1]\times[0,\tau]$. The function*

$$g(z) = \prod_{j=1}^{n} \frac{\theta(z-p_j,\tau)}{\theta(z-q_j,\tau)}$$

has the following properties

1. $g(z)$ *has a simple zero at* p_j
2. $g(z)$ *has a simple pole at* q_j
3. $g(z+1) = g(z)$
4. $g(z+\tau) = e^{2\pi i\sum_{j=1}^{n}(p_j-q_j)}g(z)$

[Wey06]

Proof. We will prove properties 3 and 4. From 2.3.0.18, we have

$$\begin{aligned} g(z+1) &= \textstyle\prod_{j=1}^{n} \frac{\theta(z+1-p_j,\tau)}{\theta(z+1-q_j,\tau)} \\ &= \frac{(-1)^n}{(-1)^n}\textstyle\prod_{j=1}^{n} \frac{\theta(z-p_j,\tau)}{\theta(z-q_j,\tau)} \\ &= g(z) \end{aligned}$$

and

$$\begin{aligned} g(z+\tau) &= \prod_{j=1}^{n} \frac{\theta(z+\tau-p_j,\tau)}{\theta(z+\tau-q_j,\tau)} \\ &= \prod_{j=1}^{n} \frac{-e^{-2\pi i\left(z-p_j+\tau/2\right)}}{-e^{-2\pi i\left(z-q_j+\tau/2\right)}} \frac{\theta(z-p_j,\tau)}{\theta(z+-q_j,\tau)} \\ &= e^{2\pi i \sum_{j=1}^{n}(p_j-q_j)} g(z). \end{aligned}$$

□

If

$$\sum_{j=1}^{n} (p_j - q_j)$$

is an integer, we have that g is a periodic function in the τ direction. Hence, we have built a function with the properties we desire.

2.4 Triply Periodic Minimal Surfaces

A special class of minimal surfaces are that we will focus on are called triply periodic minimal surfaces. This section is devoted to some important theorems involving triply periodic minimal surfaces. We also create a partial classification of these surfaces.

Definition 2.4.0.20. *An $n-$torus is the set*

$$\mathbb{T}^n = \underbrace{S_1 \times S_1 \times ... \times S_1}_{n \ \ times}.$$

Definition 2.4.0.21. *A closed Riemann surface X is called periodic if it can be conformally minimally immersed in a flat (zero principal curvature everywhere) torus $\mathbb{T}^3$. [Mee90]*

Since we want our surface to be triply periodic, we want the surface to be invariant under a group of translations in $\mathbb{R}^3$. A lattice is a group of translations and we would like points on our surface to be invariant when acted upon by elements in the lattice. We now present the definition of a triply periodic minimal surface.

Definition 2.4.0.22. *Let Λ be a lattice generated by the linearly independent vectors $v_1, v_2, v_3 \in \mathbb{R}^3$. A minimal surface M is called triply periodic if M is invariant when acted upon by Λ.*

When we take the quotient $\mathbb{R}^3/\Lambda$, we get a fundamental piece of the surface. The surfaces we are interested in will be genus 3 triply periodic minimal surfaces which can be embedded in Euclidean space. We would like to relate these surfaces to Riemann surfaces.

Lemma 2.4.0.23. *Let X be a Riemann surface and $f : X \to \mathbb{R}^3$ be a minimal surface. The zeros of the Gaussian curvature are the branch points of the Gauss map. [Mee90]*

Lemma 2.4.0.24. *If X is a Riemann surface and $f : X \to \mathbb{R}^3/\Lambda$ is a triply periodic minimal surface of genus $g \geq 1$, then the Gauss map is a $(g-1)$-sheeted conformal branched cover of sphere. [Mee75]*

In particular, this lemmas implies that a Riemann surface is hyperelliptic if $g = 3$.

Corollary 2.4.0.25. *Let X be a compact Riemann surface of genus g and $f : X \to \mathbb{T}^3$ be a minimal surface. Then the Gauss map represents X as a two sheeted branched cover of S^2. [Mee90]*

Using these lemmas, we can prove the following theorem.

Theorem 2.4.0.26. *Let X be a connected, complete, embedded, non-flat triply periodic minimal surface in $\mathbb{R}^3$ invariant under the action of a lattice Λ. Then the genus of X/Λ is at least 3.*

Proof. By previous theorem, X is a $(g-1)$ degreed cover of S^2. If $g = 2$, then X is a degree one cover of S^2, making X homeomorphic to a sphere. This would mean the surface has genus 0. If $g = 1$, then Gauss-Bonnet tells us that $\int_X K\, dA = 0$. Since X is minimal, $K \leq 0$, thus $K = 0$. This would imply X is flat. If $g = 0$, then Gauss-Bonnet tells us that $\int_X K\, dA = 2$, thus X cannot be minimal. Hence $g \geq 3$. □

This lemma shows that if a surface is triply periodic and possess some other reasonable properties, then is must have a genus of at least three. There are surfaces of higher genus, but we will not discuss them for simplicity. For more information on higher genus triply periodic minimal surfaces, I refer the reader to [Tra08].

2.4.1 Partial classification of surfaces admitting an order 2 rotation

We would like to do a classification of the surfaces we are interested in studying in this thesis. In this section, our goal is to classify all embedded triply periodic minimal surfaces of genus 3 that admit an order 2 rotational symmetry.

Theorem 2.4.1.1. *Let X/Λ be an embedded genus 3 triply periodic minimal surface invariant under an order 2 rotation ρ. Then, the genus of $X/\Lambda/\rho$ is 1.*

To prove this, we first need the following definition and a few theorems.

Definition 2.4.1.2. *Let $f : X' \to X$ be a non-constant holomorphic mapping between two compact Riemann surfaces X' and X. Let g be the genus of X' and γ be the genus of X. We define the degree of f as the cardinality of $f^{-1}(z)$ for almost all $z \in X$. [FK92]*

Theorem 2.4.1.3. *(Riemann-Hurwitz formula) Let $f : X' \to X$ be a non-constant holomorphic map between Riemann surfaces a compact Riemann surface X' of genus g and a compact Riemann surface X with genus γ. Let the degree of f be n. Define the total branching number of the mapping to be $B = \sum_{P \in X'} b_f(P)$. Then*

$$g = n(\gamma - 1) + 1 + \frac{B}{2}. \tag{2.17}$$

[FK92]

Corollary 2.4.1.4. *Assume the conditions given by Theorem 2.4.1.3. Let $T \neq 1$ e an*

automorphism on X. Define $Fix(T)$ to be the number of points left fixed under T. Then

$$|Fix(T)| \leq 2 + \frac{2g}{Order(T) - 1} + \frac{2\gamma Order(T)}{Order(T) - 1}.$$

Equality holds if and only if $order(T)$ is prime. [FK92]

Corollary 2.4.1.5. *Assume the conditions given by Theorem 2.4.1.3 and Corollary 2.4.1.4. Then*

$$2g - 2 = Order(T)(2\gamma - 2) + \sum_{j=1}^{Order(T)-1} Fix(T^j).$$

[FK92]

Now we have the tools to prove Theorem 2.4.1.1.

Proof. Let $f : X/\Lambda \to X/\Lambda/\rho$ be the quotient map. From Riemann-Hurwitz, we have

$$2 = n(\gamma - 1) + \frac{B}{2}$$

and Corollary 2.4.1.5 shows

$$8 = 4\gamma + |Fix(\rho)|$$

If $\gamma \geq 3$, then Corollary 2.4.1.5 tells is that $Fix(\rho) < 0$, which is not possible. Since $\gamma < 3$, we have from Corollary 2.4.1.5 that the fixed point set is finite. Since ρ is an order two rotation, the degree of f is two. If $\gamma = 2$, then Riemann-Hurwitz gives us that B must be zero. If B is zero, then f is unbranched, which is impossible since the order of the rotation is 2. If $\gamma = 0$, then the surface has no holomorphic one forms [FK92]. The height differential dh is invariant under ρ, thus it is a holomorphic one form and shows a contradiction. Hence $\gamma = 1$. □

The next lemma tell us the number of poles for the surfaces we are classifying.

Lemma 2.4.1.6. *Let X/Λ be an embedded genus 3 triply periodic minimal surface invariant under an order 2 rotation. The square of the Gauss map G^2 has two single order*

poles. [Wey06]

The following theorem gives us our desired classification.

Theorem 2.4.1.7. *Let M/Λ be a triply periodic minimal surface with an order 2 symmetry so that the quotient is a torus. If the quotient is fixed under the involution $-id$ centered at $\frac{1}{2}+\frac{\tau}{2}$, then the four branch points are at $0,\frac{1}{2},\frac{\tau}{2}$, and $\frac{1}{2}+\frac{\tau}{2}$. [Wey06]*

Proof. By 2.4.1.7, we know that the branch points must be $0,\frac{1}{2},\frac{\tau}{2}$, and $\frac{1}{2}+\frac{\tau}{2}$. Without loss of generality, let $g(0)=0$. Let z be the other zero and p_1 and p_2 be the two poles. Then

1. If $z=\frac{\tau}{2}$, $p_1=\frac{1}{2}$, and $p_2=\frac{1}{2}+\frac{\tau}{2}$ then we get the tP family. We further discuss this family in 3.1.

2. If $z=\frac{1}{2}$, $p_1=\frac{\tau}{2}$, and $p_2=\frac{1}{2}+\frac{\tau}{2}$ then we get the tD family. We further discuss this family in 3.2.

3. If $z=\frac{1}{2}+\frac{\tau}{2}$, $p_1=\frac{1}{2}$, and $p_2=\frac{\tau}{2}$ then we get the $tCLP$ family. We further discuss this family in 3.3.

□

2.4.2 Partial classification of surfaces admitting an order 3 rotation

In this section, our goal is to classify all embedded triply periodic minimal surfaces of genus 3 that admit an order 3 rotational symmetry. The ideas of this section are similar to the last section, except we are now looking a surfaces with an order 3 rotation.

Lemma 2.4.2.1. *Let M be a hyperelliptic Riemann surface with $\rho \in Aut(M)$ of order 3. Then every fixed point of ρ is a hyperelliptic point. [FK92]*

Lemma 2.4.2.2. *The cube of the Gauss map g^3 has a double order pole at p and a double order zero at 0. Furthermore, $p=\frac{1}{2},\frac{\tau}{2}$, or $\frac{1}{2}+\frac{\tau}{2}$.*

Theorem 2.4.2.3. *Let M be an embedded triply periodic minimal surface of genus 3 that admits a rotational symmetry of order 3 about an axis $L \in \mathbb{R}^3$. Assume that $M\Lambda$ admits a reflection in a plane containing L so that the fixed point set in $M/\Lambda/\rho$ consists of two components. Then M is a member of the rPD or rH families. [Wey06]*

Proof. We know that g^3 has exactly 3 two branch points. Without loss of generality, let $g(0) = 0$ The location of the other branch point p must be:

1. If $p = \frac{1}{2}$, this data generates the rH family. We discuss this family in 3.4.
2. if $p = \frac{1}{2} + \frac{\tau}{2}$, this data generates the rPD family. We discuss this family in 3.5.
3. If $p = \frac{\tau}{2}$, then this data is associated to the H family and it cannot be embedded. [Wey06]

□

CHAPTER 3

EXAMPLES OF TRIPLY PERIODIC MINIMAL SURFACES

In the previous section, we classified a group of embedded triply periodic minimal surfaces that are invariant under order 2 rotations and surfaces invariant under 3 rotations. We now discuss these surfaces in a little more depth and also introduce some related surfaces to the ones classified.

3.1 Schwarz tP Family

The Schwarz P surface (which we will just call the P Surface) was discovered by H.A. Schwarz in 1890 [Sch90]. The P surface is a very interesting surface to study because of its symmetry. When we discussed the P surface in the previous section, the surface was built with an order 2 rotation axes parallel to the x_3 axis and a mirror plane perpendicular to this rotation axis. If we vary the parameter τ in the Gauss map, we get a whole family of minimal P surfaces. The "most symmetric" P surface has the following symmetries:

- An order two rotational symmetry about the x_1, x_2, and x_3 axes.
- An order two rotational symmetry about an axis in the x_1, x_2 plane containing the point $(1, 1, 0)$.
- An order three rotational symmetry about the line containing the origin and the point $(1, 1, 1)$. There are three more rotations that intersects the corners of the cubic lattice that are similar to this.
- An order four rotational symmetry about each of the coordinate axes.

- A reflectional symmetry in each plane containing x_i and x_j, $i \neq j$. There are three of these in total.
- An additional three reflectional symmetries. Each reflection is through a plane containing the x_i axis and a fixed Weierstrass point.
- Rotation of π about any of the straight lines it contains. [Wey06]

If $I(P)$ denotes the isometry group of the P surface, we get that $|I(P)| = 96$ [Mee75]. It can also be shown that the P surface has the largest isometry group compared to any genus 3 triply periodic minimal surface (except the D surface, which has the same amount of elements) [Mee75]. We will be using these symmetries later to help compute the surface area of these surfaces. The square of the Gauss map of the P surface is given by

$$g^2(z) = \frac{\theta(z, ai)\,\theta\left(z - \frac{a}{2}i, ai\right)}{\theta\left(z - \frac{1}{2}, ai\right)\theta\left(z - \frac{1+ai}{2}, ai\right)},$$

where $a > 0$ and the height differential $dh = dz$ [Wey06]. We can check that the Gauss map is in fact doubly periodic. Using Lemma 2.3.0.19, we can see that $g(z+1) = g(z)$ and

$$\begin{aligned} g(z + ai) &= \sqrt{e^{2\pi i \sum_{j=1}^{2}(p_j - q_j)}}\, g(z) \\ &= \sqrt{e^{-2\pi i}}\, g(z) \\ &= g(z). \end{aligned}$$

Hence, the Gauss map is doubly periodic. One question we may have is whether or not this Gauss map is unique. The following proposes that the Gauss map is unique up to a constant.

Proposition 3.1.0.4. *Let $g_1(z)$ be the square of the Gauss map as defined above. Let $g_2(z)$ be another meromorphic function with the same simple zeros on poles, $g_2(z+1) =$*

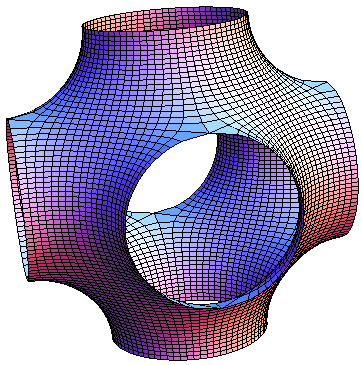

Figure 3.1: A Translational Fundamental Domain of the P Surface

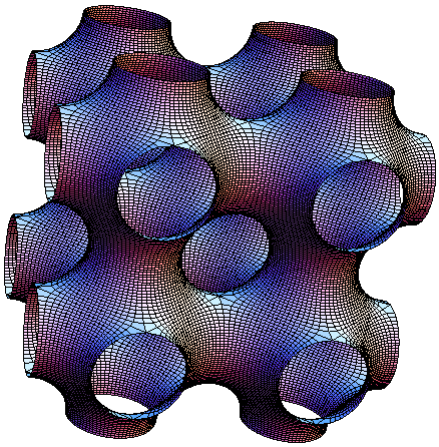

Figure 3.2: Multiple Translational Fundamental Domains of the P Surface

$g(z)$, $g(z+\tau) = g(z)$, the same two single order poles as $g_1(z)$, and the same two single order zeros as $g_1(z)$. Then g_1 and g_2 differ by a constant factor.

Proof. Define a function $h(z) := g_1(z)/g_2(z)$. Since

$$\begin{aligned} h(z+1) &= \frac{g_1(z+1)}{g_2(z+1)} \\ &= \frac{g_1(z)}{g_2(z)} \\ &= h(z) \end{aligned}$$

and $h(z+\tau) = h(z)$, h is doubly periodic. For $i = 1, 2$, each g_i is meromorphic with simple zeros and poles. By definition of a simple zero and a pole, for each each g_i there

exist a holomorphic functions g_i^* such that

$$g_i(z) = g_i^*(z)\frac{(z-z_1)(z-z_2)}{(z-p_1)(z-p_2)}.$$

This shows that $h(z) = g_1^*(z)/g_2^*(z)$. We first note that h is holomorphic since $g_1^*(z)$ and $g_2^*(z)$ have no zeros or poles. By Proposition 2.3.0.17 , h is constant. □

The parameter in the Gauss map ai can be written as τ, where $\tau \in i\mathbb{R}$. When $\tau \approx 0.781701$, we get the most symmetric P surface. The exact value τ that makes the most symmetric P surface can be computed by integrating some lovely elliptic integrals (See [Wey06]). If we vary τ, we get a family of P surfaces. We call this family the tP family, where the t means tetragonal. We will discuss this concept more in a later sections, when we discuss symmetries on these surfaces.

Looking at Figure 3.2, we can see the triply periodic behavior of the surface. This shape can be called "The Plumber's Nightmare" since we have a series of tubes in three directions. We may be able to imagine ourselves as water traveling inside these tubes in any direction, but not being able to break outside the tubes without crossing through the surface. This separation of space into two regions is a core subject of this thesis and will be discussed more in depth later in this thesis.

3.2 Schwarz tD Family

In the associate family of the P surface, we get two embedded triply periodic minimal surfaces. When we multiply the height differential of the P surface by $e^{\pi i/2}$, we get the Schwarz D surface. Like the P surface, the D surface was discovered by of H.A. Schwarz [Sch90]. The square of the Gauss map of the D surface is given by

$$g^2(z) = \frac{\theta(z, ai)\,\theta\left(z - \frac{a}{2}i, ai\right)}{\theta\left(z - \frac{1}{2}, ai\right)\theta\left(z - \frac{1+ai}{2}, ai\right)},$$

where $a > 0$ and the height differential $dh = e^{\frac{i\pi}{2}}dz$ [Wey06].

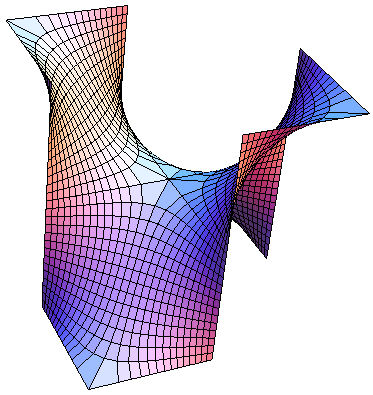

Figure 3.3: A Translational Fundamental Domain of the D Surface

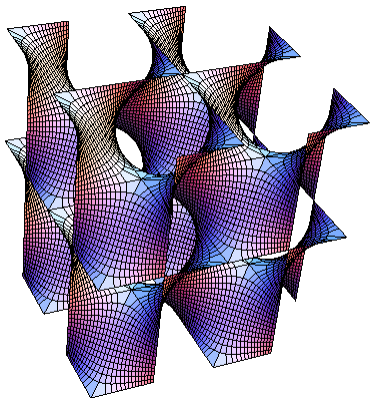

Figure 3.4: Multiple Translational Fundamental Domains of the D Surface

Just like the P surface, the most symmetric D surface is formed when $\tau \approx 0.781701i$, which gives us a D surface with the same number of elements in the isometry group as the P surface [Wey06]. Varying the parameter τ, we get a family of D surfaces called the tD family. One problem that the D surface has that we do not encounter from the P surface is an orientation problem when looking at translational fundamental domains of the surface. The picture in Figure 3.5 attempts to illustrate this problem. If we make a choice of normal, it will not be preserved if we move over one translation. I encourage the reader to use the Mathematica notebook for the D surface to see this problem more clearly for themselves. We can solve this problem by calling the surface shown in Figure 3.4 one translational fundamental domain of the surface instead. We then can give the surface a consistent choice of normal.

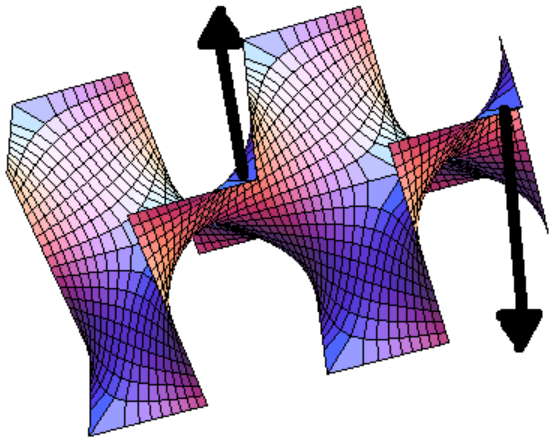

Figure 3.5: Using one fundamental domain, we cannot make a consistent choice of normal.

3.3 Schwarz CLP Family

The final surface that we will describe with an order 2 symmetry is the CLP surface. The square of the Gauss map of the CLP surface is given by

$$g^2(z) = \frac{\theta(z, ai)\,\theta\left(z - \frac{1}{2} - \frac{a}{2}i, ai\right)}{\theta\left(z - \frac{1}{2}, ai\right)\,\theta\left(z - \frac{a}{2}i, ai\right)},$$

and $dh = dz$ [Wey06].

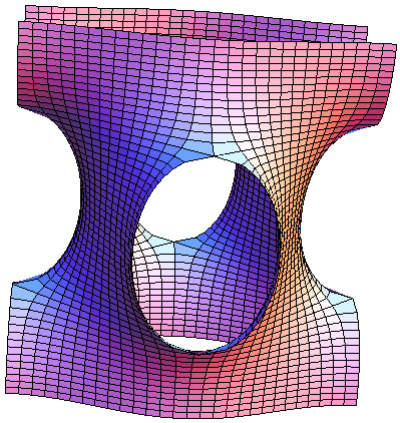

Figure 3.6: A Translational Fundamental Domain of the CLP Surface

If we vary the parameter τ, we get a family of minimal CLP surfaces. We will not mention as much about the CLP surfaces since they have less symmetry than the other order 2 surfaces.

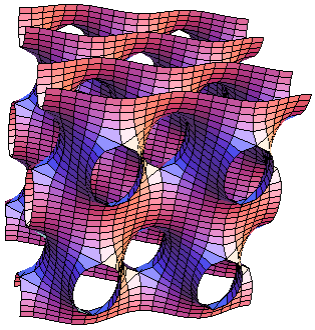

Figure 3.7: Multiple Translational Fundamental Domains of the CLP Surface

3.4 Schwarz H Family

When we classified surfaces with an order 3 symmetry, we first came up with the Schwarz H surface [Sch90]. The cube of the Gauss map of the Schwarz H surface is defined as

$$g^3(z) = \left(\frac{\theta(z, ai)}{\theta\left(z - \frac{1}{2}, ai\right)} \right)^2$$

with $dh = dz$ [Wey06].

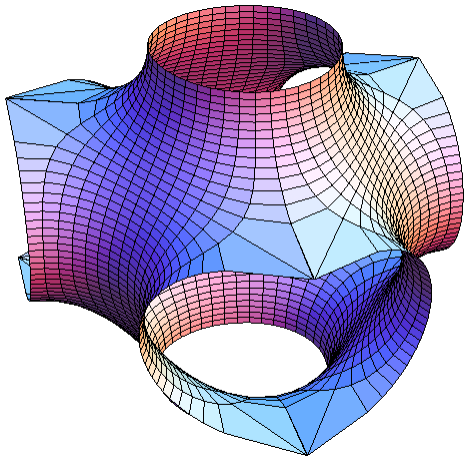

Figure 3.8: A Translational Fundamental Domain of the H Surface

The H surface has an order 3 rotation axes with a reflection plane perpendicular to that rotation axes. The H surface sits in an hexagonal prism lattice. Each member of the rH family contains straight lines that form an equilateral triangle on the surface. Unlike the tP family, the rH family does not have a "most symmetrical" member.

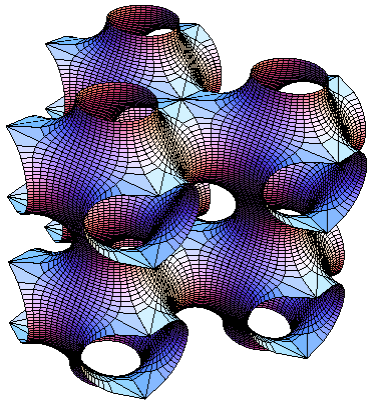

Figure 3.9: Multiple Translational Fundamental Domains of the H Surface

3.5 Schwarz rPD Family

The next order three surface we classified is the PD surface [Sch90]. The cube of the Gauss map of the rPD surface is defined as

$$g^3(z) = \left(\frac{\theta(z, ai)}{\theta\left(z - \frac{ai}{2} - \frac{1}{2}, ai\right)} \right)^2$$

and the height differential is $dh = e^{\pi i/2} dz$.

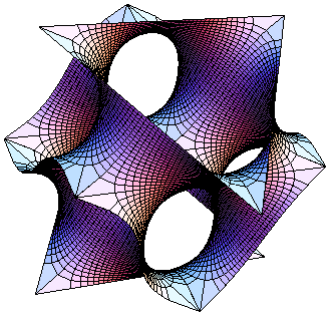

Figure 3.10: A Translational Fundamental Domain of the PD Surface

The PD surface can be obtained by looking at the P surface from an order 3 perspective. [Wey06]

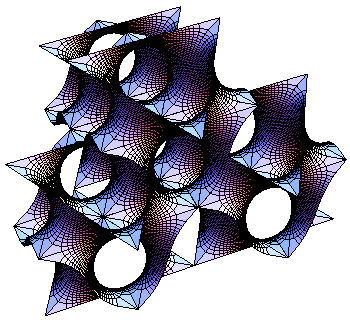

Figure 3.11: Multiple Translational Fundamental Domains of the PD Surface

3.6 The Gyroid

As mentioned before, there were two embedded members in the associate family of the P surface. The D surface is related to the P surface by multiplying the height differential of the P surface by $e^{\pi i/2}$. The other embedded surface in the P surface associate family is called the gyroid. The gyroid is sometimes called the Schoen G surface. The gyroid was discovered by Alan Schoen in 1970 [Sch70]. If we multiply the height differential of the P surface by $e^{\theta i}$, where $\theta \approx 0.663482971$, we get the height differential of the gyroid. It is slightly odd that this value for θ is the only value of θ between 0 and $\pi/2$ that gives us an embedded surface. Schoen did not prove the surface was embedded; however, the gyroid was finally proven to be an embedded surface in [GBW96]. The square of the Gauss map of the gyroid is given by

$$g^2(z) = \frac{\theta(z, ai)\,\theta\left(z - \frac{a}{2}i, ai\right)}{\theta\left(z - \frac{1}{2}, ai\right)\theta\left(z - \frac{1+ai}{2}, ai\right)},$$

where $a > 0$ and the height differential $dh = e^{i\theta}dz$ ($\theta \approx 0.663482971$).

The gyroid has an order 3 rotational symmetry. There exists a family of minimal gyroids with an order 3 rotation that can be found by varying the parameter $\tau \in \mathbb{C}$ a certain way [Wey06], though it is not known for certain what these exact values are. There are different ways to view they gyroid. The gyroid can be viewed in as a surface with a cubic lattice; however, it is a genus 5 surface when viewed from this perspective [Ros03]. Instead, we view the gyroid in a rhombohedral lattice. This way, we get a genus

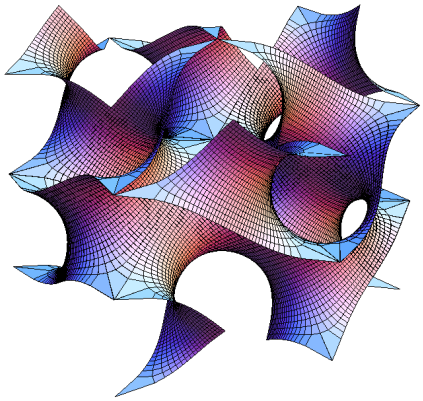

Figure 3.12: A Translational Fundamental Domain of the Gyroid

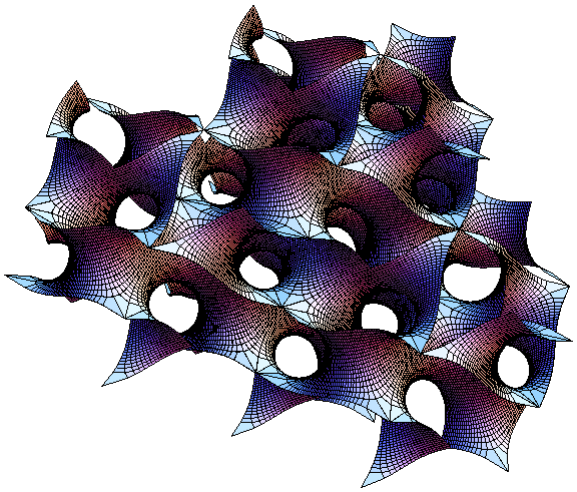

Figure 3.13: Multiple Translational Fundamental Domains of the Gyroid

3 surface. This can be shown using Gauss-Bonnet. The entire family of gyroids sit in a rhombohedral lattice. One interesting property of the gyroid is that there are no straight lines on the surface [GBW96]. The symmetries of this family will be discussed in later on in the thesis.

3.7 The Lidinoid

Like the P surface, the H surface's height differential can be multiplied by a factor to make an embedded minimal surface. If we multiply the height differential of the H surface by $e^{\theta i}$, where $\theta \approx 1.12067$, we get an embedded minimal surface called the Lidinoid. The Lidinoid was discovered by Sven Lidin in 1990 [LL90]. The surface was proved to be an

embedded surface by Karsten Große-Brauckmann and Meinhard Wohlgemuth in 1996 [GBW96]. The cube of the Gauss map of the Lidinoid is

$$g^3(z) = \left(\frac{\theta(z, ai)}{\theta\left(z - \frac{1}{2}, ai\right)} \right)^2$$

and the height differential is $dh = e^{i\theta} dz$, where $\theta \approx 1.12067$.

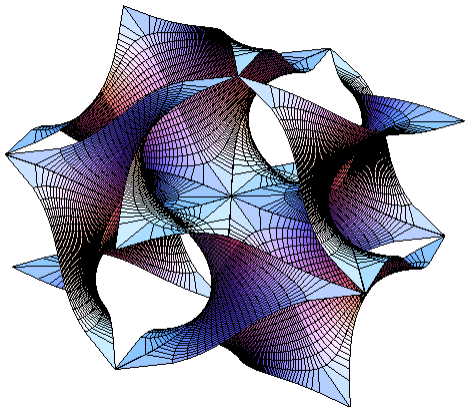

Figure 3.14: A Translational Fundamental Domain of the Lidinoid

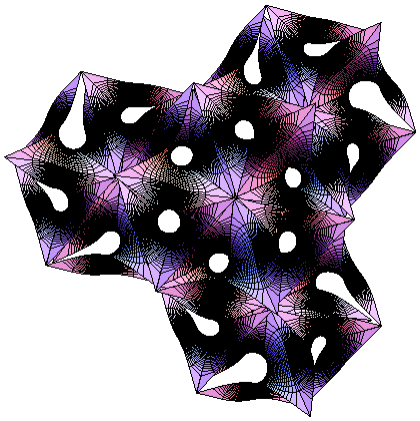

Figure 3.15: Multiple Translational Fundamental Domains of the Lidinoid

Like the gyroid, the Lidinoid contains no straight lines on it's surface. We can vary $\tau \in \mathbb{C}$ to obtain a family of minimal Lidinoids [Wey06]. The existence of this family is known; however, specific values of τ that make the family are unknown [Wey06]. It is also conjectured that the gyroid and Lidinoid share a family (personal communication from Adam Weyhaupt).

CHAPTER 4

ISOPERIMETRIC PROPERTIES

Let N be a 3-dimensional Riemaniann manifold with positive and finite volume $V(N)$. We would like to know if there exist a compact surface $M \subset N$ such that M encloses a region $V(N)/2$ and M minimizes surface area under certain constraints. We also would like to know if the genus three embedded triply periodic minimal surface we have discussed are possible solutions to this problem. The goal of this section is to show that under some assumptions, an embedded triply periodic minimal surface has an "inside" and an "outside" and each region has equal volume.

Definition 4.0.0.5. *Let X be a hyperelliptic Riemann surface. The hyperelliptic involution is the automorphism $\iota : X \to X$, that maps the point (x, y) to $(x, -y)$ [Mee75].*

This hyperelliptic involution interchanges the sheets on the Riemann surface. To the prove the main theorem of this section, we need some prerequisites. The following lemma gives a basis for the holomorphic differentials on a hyperelliptic Riemann surface.

Lemma 4.0.0.6. *Let X be a genus g hyperelliptic Riemann surface that can be written in the form as in* (2.1)*. Then*

$$\left\{ \frac{dx}{y}, z\frac{dx}{y}, ..., x^{g-1}\frac{dx}{y} \right\}$$

forms a basis for the differentials of the first kind on X. [FK92]

The next lemma states that a minimal surface can split space into two regions under certain circumstances.

Lemma 4.0.0.7. *Let X be a complete embedded minimal surface in $\mathbb{R}^3$, then X disconnects $\mathbb{R}^3$ into two regions. [Mee81]*

We like to be able to name the regions separated by the surface. One region will be called the inside while the other will be called the outside. These terms are not well defined, so we present an appropriate definition for the two regions.

Definition 4.0.0.8. *Let X be a closed orientable surface embedding into $\mathbb{R}^3$ (or $\mathbb{R}^3/\Lambda$) such that X separates $\mathbb{R}^3$ ($\mathbb{R}^3/\Lambda$) into two disjoint regions. Let s be a point on X. Make a choice of normal. Let p be a point not on the surface. Let δ:$[0,1] \to \mathbb{R}^3$ be a continuous curve with the following properties: $\delta(0) = p$, $\delta(1) = s$, and δ maps to no other point on the surface. If in a small neighborhood around s the curve δ lies on the same side as the direction of the normal, then we say p is outside of the surface. Otherwise, p is inside the surface.*

To justify that this is a good definition, take two points p_1 and p_2 on the outside. Let δ_i be the continuous curve that connects p_i to some s_i on the surface. Make a path connected compact set that contains s_1 and s_2. Cover of this set of small balls such that each are locally a graph. Take a finite subcover. Connect s_1 and s_2 with a continuous curve. Now we can perturb this curve out by a small amount in the direction of the surface normal. Thus, we can connect p_1 and p_2 with a path. This shows that the inside and the outside are both connected sets.

Now we have a reasonable definition for the outside and inside of a surface up to a choice of normal. We now will show that a hyperelliptic triply periodic minimal surface splits its quotient space into two disjoint regions of equal volume. We will show this in two steps. First we will show that the surface separates $\mathbb{R}^3/\Lambda$. Then we will show that the regions are congruent.

Lemma 4.0.0.9. *Let X be an orientable, path connected, embedded, triply periodic minimal surface with lattice Λ that separates $\mathbb{R}^3$ into two regions. Assume p is a point on the outside (inside) of the surface. Then $p + v$ is on the outside (inside) as well, for any $v \in \Lambda$.*

Proof. Since $p \notin X$, there exist a continuous curve $g : [0,1] \to \mathbb{R}^3$ with $g(0) = p$ and

$g(1) = x$ for some $x \in X$ such that g never intersects the surface except at x. Similarly, the curve $g + v$ connects $p + v$ to $x + v$. Since X is path connected, there exists a continuous curve h that connects x with $x+v$. Since X is minimal, the surface is a graph in small balls around each point. Cover the curve h in these balls. Since h is compact, take a finite subcover. Choose the normal to point in the initial direction of g. If we push off at the normal at x , the normal will stay on the same side along h in each member of the finite subcover. We can then travel from p to $p + v$ via g, h, and $g + v$. Since the normal is consistent along h, p and $p + v$ are both on the outside. □

Theorem 4.0.0.10. *Let X be an orientable, path connected, embedded, triply periodic minimal surface with lattice Λ that separates $\mathbb{R}^3$ into two regions. Then X/Λ separates $\mathbb{R}^3/\Lambda$ into two regions.*

Proof. Assume X/Λ does not separate $\mathbb{R}^3/\Lambda$. Our goal is to find a contradiction. Take two points p and q in $\mathbb{R}^3/\Lambda$ so some lifts of those points in $\mathbb{R}^3$ are in different components. There exists a continuous curve $g : [0, 1] \to \mathbb{R}^3/\Lambda$ with $g(0) = p$ and $g(1) = q$ that does not intersect X/Λ. Choose a lift of p in $\mathbb{R}^3$. There is a unique lift of g to R^3, call it $\tilde{g}$ so that $\tilde{g}$ is continuous and $\tilde{g}(0)$ is the designated lift of p. This curve does not intersect X since g does not intersect X/Λ. Any lift of p is on the same side of some lift of q. By Lemma 4.0.0.9, all lifts are on the same side. This makes a contradiction. Hence X/Λ separates $\mathbb{R}^3/\Lambda$ into two regions. □

We now prove the volumes are congruent.

Theorem 4.0.0.11. *Let X be a genus g hyperelliptic Riemann surface and $f : X \to \mathbb{R}^3/Lambda$ be a triply periodic complete minimal embedding of X onto $f(X)$. Then $f(X)$ separates $\mathbb{R}^3/\Lambda$ into two disjoint regions of equal volume.*

Proof. Let p_0 be a hyperelliptic point. Then up to a translation

$$f(p) = \int_{p_0}^{p} (\omega_1, \omega_2, \omega_3)$$

and

$$\begin{aligned} f(\iota(p)) &= \int_{p_0}^{\iota(p)} (\omega_1, \omega_2, \omega_3) \\ &= \int_{p_0}^{p} (\iota^*(\omega_1), \iota^*(\omega_2), \iota^*(\omega_3)). \end{aligned}$$

Since $\left\{ \frac{dx}{y}, \frac{xdx}{y}, \frac{x^2dx}{y}, ..., \frac{x^{g-1}dx}{y} \right\}$ is a basis for forms on X, we have for any 1-form ω on X

$$\begin{aligned} \iota^*(\omega) &= \iota^* \left(\alpha_1 \frac{dx}{y} + \alpha_2 \frac{xdx}{y} + ... + \alpha_{g-1} \frac{x^{g-1}dx}{y} \right) \\ &= -\alpha_1 \frac{dx}{y} - \alpha_2 \frac{xdx}{y} - ... - \alpha_{g-1} \frac{x^{g-1}dx}{y} \\ &= -\omega \end{aligned}$$

for some unique scalers α_i. Thus

$$\begin{aligned} f(\iota(p)) &= -\int_{p_0}^{p} (\omega_1, \omega_2, \omega_3) \\ &= -f(p). \end{aligned}$$

Since the involution preserves the direction of the normal, the region that was previous called the inside is now on the outside. Thus, the two regions are congruent. □

To give the D surface orientation, we take the translational fundamental domain and translates it into a 2 by 2 by 2 block like in Figure 3.4. The surface become a genus 9 surface that still separates space. There is also a way to view the gyroid as a genus 5 surface with a cubic lattice and still get space separation [Ros03]. If the surface is not hyperelliptic, then we do not necessarily get this separation of space. Thus, not all higher genus surfaces will separate space. More information on hyperelliptic surfaces and their genus can be found in [FK92].

Sometimes, it is easy to see this volume splitting. In Figure 4.1, we see we can easily fit in the P surface into itself. Sometimes, may need to some more gymnastics. In Figure

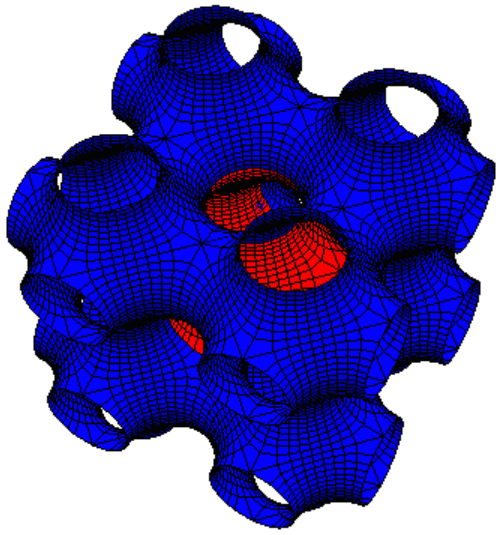

Figure 4.1: This figure shows that we can fit a copy of the P surface on the "outside" of the surface.

4.2 we need to make a rotation to fit the H surface into itself. Some picture are harder to get or see in the case of the gyroid or D surface.

The lattice of the quotient space $\mathbb{R}^3/\Lambda$ forms a parallelepiped. We can use surfaces that satisfy the previous theorem to split this parallelepiped into two section of equal volume. An interesting problem arises from this idea. What surface that splits $\mathbb{R}^3/\Lambda$ into two volumes has smallest surface area? In the case where the generating vectors of Λ are orthogonal. the answer is a pair of planes [Ros05]. Some surface we will look at have non-rectangular prism lattices. We also should note the symmetries on these surfaces. We may want to know what surface that has a certain group of symmetries and splits it's lattice in half has the smallest surface area. We should keep this idea in mind when looking at the surface areas of these surfaces in the final section of this paper.

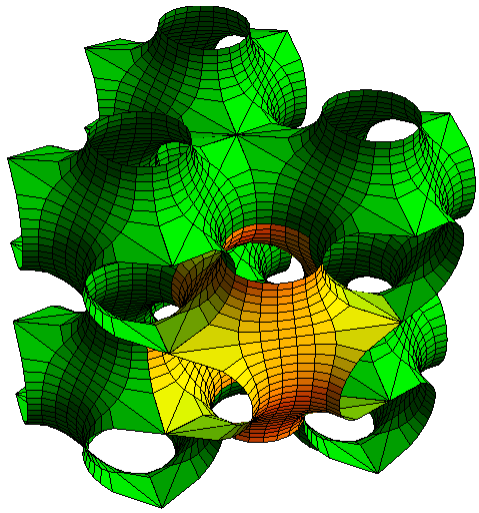

Figure 4.2: This figure shows the H surface separating space into two equal regions.

CHAPTER 5

CRYSTALLOGRAPHIC SPACE GROUPS

In the previous section, we found that genus 3 triply periodic minimal surfaces separate $\mathbb{R}^3/\Lambda$ into two regions of equal volume. Another property of these surfaces to study is the symmetries of these surfaces. Since these surfaces are of interest to chemist and biologists, we discuss basic notation from crystallography and apply it to these surfaces.

5.1 Explanation of Notation

A good reference for this notation is [San94]. A point group is a group of isometries in a lattice that leaves at least one point fixed. If we add translational symmetries to a point group, we get a space group. The lattice of the space group consists of three vectors. One vectors is the x direction, one vectors is the y direction, and one vector is the z direction. Chemists are interested in these structures because crystal form in a periodic fashion.

We will be using Hermann-Mauguin symbols to describe point groups and space group. The notation representing a space group is in the form $A_1a_2a_3a_4$, where A_1 describes the lattice, and the other symbols describe the elements of the group.

Each surface has translational symmetry when we translate it by a lattice vector. A lattice that contains no other translational symmetry is called a primitive lattice and we denote space groups with the letter P. Space groups with the translational symmetries $(x + 1/2, y, z)$, $(x, y + 1/2, z)$, and $(x, y, z + 1/2)$ are called face-centered and we denote these groups with the letter F. Space groups with the translational symmetry with the translation $(x + 1/2, y + 1/2, z + 1)/2$ are called body-centered and are denoted by the letter I.

Rotations are given by a positive integer n. An order n rotation would be given an n. Groups we will be looking will have either an order 2,3,4, or 6 rotation. It can be shown that these are the only type of rotations that can occur for crystallographic space groups [San94]. An improper rotation that consists of a rotation of $2\pi/n$ followed by an inversion through a point on the rotation axis is given the symbol $\bar{n}$. The letter m represents a reflection across that plane that is normal to a direction. For a positive integer n, the notation n/m is one component of the notation and means there is a mirror plane perpendicular to an order n rotation axis. There is also notation to describe isometries that do not leave points fixed. A screw rotation given by a rotation of $2\pi/n$ followed by a translation of p/n in some direction ($p \in \mathbb{N} < n$) is given by the symbol n_p. Glide planes are reflections in a plane followed by a translation parallel to the reflection plane. If the glide reflection is in the x direction, the letter a is used to represent the reflection followed by a translation of $x/2$. Similarly, b represents the y directions and c represents the z direction. A diagonal glide; given by the letter n (not to be confused with a rotation where a number will appear) is a translation in the direction $(x + y)/2$, $(x + z)/2$, $(y + z)/2$. In some lattices, there can be a diagonal glide reflection in the $(x + y + z)/2$ direction as well. A diamond glide reflection is given the letter d has a translation $(x \pm y)/4$, $(x \pm z)/4$, or $(y \pm z)/4$ or in some cases for some cases $(x \pm y \pm c)/4$.

Each lattice can take on a different shape. Depending on the shape, the symbols in different positions will mean different things. There are possible lattices: triclinic, orthorhombic, tetragonal, trigonal (rhombohedral), hexagonal, and cubic. We will describe the notation for the cubic, tetragonal, hexagonal, and special class of the trigonal lattices called rhombohedral lattices. We choose these types of lattices to discuss because the surfaces we classified have a lattice of one of these types.

5.2 Cubic Space Groups

The first type of space group we discuss is the cubic space group. The lattice is generated by three orthogonal vectors of equal length (a cube). The notation is given as a sequence of letters and numbers. The first component will be a letter describing the translational symmetry, e.g. P,F, or I. The second component refers to the cube's edges. The third component in the cubic space group notation will have the symbol 3 or $\bar{3}$ and refers to the four body diagonals of the cube. The final component refers to the face diagonals. The final component is not always required for cubic space groups. When we have a screw rotation, we replace the rotation symbol with the symbol for a screw rotation. An m in the point group notation may sometimes be replaces by a glide reflection in the space group. An example is the cubic space group $Pm\bar{3}m$. The notation tells us that the space group has a primitive lattice, mirror planes normal to the x,y, and z axes, an order 3 improper rotation about the body diagonals, and mirror planes normal to the face diagonals.

The most symmetric P and D surface both have a cubic lattice. Based on their symmetries we would like to know which space groups these surfaces belong to. The space groups for the P surface are given in this next theorem.

Theorem 5.2.0.12. *The most symmetric P surface (as mentioned in the P Family section) has the following space groups: $P23$, $Pm\bar{3}$, $P432$, $P\bar{4}3m$, and $Pm\bar{3}m$.[Ros03]*

The final space group $Pm\bar{3}m$ has 48 elements. Space groups; at most, are limited to 48 elements, making this group one of the most symmetric groups. The next theorem gives the space groups for the most symmetric D surface.

Theorem 5.2.0.13. *If we take the most symmetric D surface and make a 2 by 2 by 2 block of the translational fundamental domain, then this surface has the following space groups: $F23$, $Fm\bar{3}$, $F\bar{4}3m$, $F4_132$, $Fd\bar{3}$, $F\bar{4}3c$, $Fd\bar{3}m$, $Fm\bar{3}c$, and $Fd\bar{3}c$. [Ros03]*

5.3 Tetragonal Space Groups

When we vary the parameter τ in the P and D surface, we no longer get a cubic lattice. A tetragonal space group is similar to a cubic space group, except the z direction is not required to be the same length as the x and y directions. The lattice is then shaped like a rectangular prism. The first component in the notation describes the translational symmetry. The second component is always a 4 or $\bar{4}$ and refers to the a rotation axis in the z direction. The third component refers to the x and y axes. The final component refers to the two directions in the xy plane that bisects the x and y axes. An example of a tetragonal space group is $P4/mmm$. The notation tells us that the space group has a primitive lattice, a fourfold rotation axes in the z direction, a mirror plane perpendicular to the z axes, mirror planes normal to the x and y axes, and a mirror plane normal to the line that bisects the x and y axes in the xy plane.

The P surfaces that are not the most symmetric have are examples of surfaces having a tetragonal lattice.

Conjecture 5.3.0.14. *Members of the tP family that are not the most symmetric P have the following space groups:* $P4$, $P\bar{4}$, $P4/m$, $P422$, $P4mm$, $P\bar{4}2m$, *and* P/mmm.

5.4 Hexagonal Space Groups

In a hexagonal space group, two of the lattice generating vectors make a 120 degree angle, while the vector in the z direction is orthogonal to the other two vectors. Once again, the first component of the notation is a P,I, or a F. The second component is a 6 or $\bar{6}$ and refers a rotation axis in the z axis direction. The third component refers to the plane normal to the 6 or $\bar{6}$ direction. The last component refers to the direction that bisects the angle between the two generating vectors that make an 120 degree angle with each other. An example would be the hexagonal space group $\bar{6}m2$. This group has an order 6 improper rotation axis parallel to the z direction, mirror planes in other two directions intersection at the previous rotation axes, and an order 2 rotation axes that

bisects the vectors that are 120 degrees apart.

The lattice for each H family members are hexagonal. All members of the family have the space groups given in the following theorem.

Theorem 5.4.0.15. *The family has the following hexagonal space groups: $P\bar{6}$, $P\bar{6}m2$, and $P\bar{6}2m$.*

Proof. We know surfaces in H family have an order 3 rotation exist in the z direction and a mirror plane normal to this axis. We must prove that the H surface has a $\bar{6}$ symmetry. Translate the surface so that order 3 rotation axis passes through the origin and the reflection plane is the xy-plane. Fix z. Rotate the point about the order 3 rotation axis, then reflect it across the mirror plane. Hence, we have the inversion we desire. □

5.5 Rhombohedral Space Groups

The generating vectors of a rhombohedral space group are of equal length. These three generating vectors v_1, v_2, v_3 are also 120 degrees apart from each other. Rhombohedral space groups are a subset of trigonal space groups. For this reason, the first component of the notation will be the letter R. The second component is a 3 or $\bar{3}$ and refers a rotation axis in the $v_1 + v_2 + v_3$ direction. An optional third component will symmetries related to the plane normal to the rotation axis. For example, the space group $R3m$ has a mirror plane perpendicular to the order 3 rotation axis.

The PD, gyroid, and Lidinoid families have a rhombohedral lattice. By construction, the PD family has the space groups $R3$ and $R3m$. The gyroid and Lidinoid also have these space groups. Members of the gyroid and Lidinoid families that are not the Lidinoid and gyrpod admit the order 3 rotation but do not have the mirror plane normal to the rotation axis.

CHAPTER 6

SURFACE AREA RESULTS

In this thesis, we are interested in surfaces that separate $\mathbb{R}^3/\Lambda$ into two regions of equal volume. In the case where $\mathbb{R}^3/\Lambda$ is a cubic lattice, the solution to this problem is a pair of planes [Ros03]. We can also add restrictions on the separating surfaces such as requiring certain symmetries. Then, planes are no longer a solution depending on the required symmetry.

Definition 6.0.0.16. *A map $F : U \subset \mathbb{R}^2 (or\ \mathbb{C}) \to \mathbb{R}^3$ is called conformal if for all $p \in U$ and all tangent vectors u, y on U*

$$\langle F_u, F_v \rangle = \lambda^2 \langle u, v \rangle ,$$

where $\lambda > 0$ is called the conformal factor. [Web04]

Theorem 6.0.0.17. *If $F : U \subset \mathbb{R}^2 (or\ \mathbb{C}) \to \mathbb{R}^3$ is a minimal map, then F is conformal. [Web04]*

Since minimal maps are conformal [Web04], we get the following proposition.

Proposition 6.0.0.18. *Let $F : U \subset \mathbb{R}^2 \to \mathbb{R}^3$ be a minimal map. The surface area of the minimal surface is*

$$\iint_U \lambda^2 \, dudv,$$

where λ is the conformal factor.

Proof. First, take u and v to be orthonormal vectors in the tangent plane of the surface. We rewrite the squared norm of $F_u \times F_v$ as

$$|F_u \times F_v|^2 = \langle F_u \times F_v, F_u \times F_v \rangle .$$

The inner product can then be rewritten as

$$\begin{aligned}
\langle F_u \times F_v, F_u \times F_v \rangle &= \langle F_u, F_v \times (F_u \times F_v) \rangle \\
&= \langle F_u, \langle F_v, F_v \rangle F_u - \langle F_v, F_u \rangle F_v \rangle \\
&= \langle F_u, \langle F_v, F_v \rangle F_u \rangle - \langle F_u, \langle F_v, F_u \rangle F_v \rangle \\
&= \langle F_v, F_v \rangle \langle F_u, F_u \rangle - \langle F_v, F_u \rangle \langle F_u, F_v \rangle \\
&= \langle F_v, F_v \rangle \langle F_u, F_u \rangle - \langle F_v, F_u \rangle^2 .
\end{aligned}$$

Since our map is conformal, we have the relation

$$\lambda^2 \langle u, v \rangle = \langle F_u, F_v \rangle .$$

Thus

$$\begin{aligned}
\langle F_v, F_v \rangle \langle F_u, F_u \rangle - \langle F_v, F_u \rangle^2 &= \langle dF(v), dF(v) \rangle \langle dF(u), dF(u) \rangle - \langle dF(v), dF(u) \rangle^2 \\
&= \lambda^4 \langle v, v \rangle \langle u, u \rangle - \lambda^4 \langle v, u \rangle \\
&= \lambda^4 \left(|v|^2 |u|^2 - \langle v, u \rangle \right) .
\end{aligned}$$

Since $|v| = |u| = 1$ and $v \perp u$, we have

$$\lambda^4 \left(|v|^2 |u|^2 - \langle v, u \rangle \right) = \lambda^4 .$$

Thus

$$\begin{aligned}
\iint_U |F_u \times F_v| \, dudv &= \iint_U \sqrt{\lambda^4} \, dudv \\
&= \iint_U \lambda^2 \, dudv .
\end{aligned}$$

□

Lemma 6.0.0.19. *If $f : X \to \mathbb{R}^3$ is a minimal surface, then*

$$\lambda^2 = \frac{1}{2}\left(\left|\left(1-g^2\right)\right|^2 + \left|\left(1+g^2\right)\right|^2 + 4\left|g\right|^2\right).$$

We would like to compare the surface area of each surface to the volume of the lattice. Since the scale of volume and surface area differ, we need to normalize the ratio between them so we can properly compare them. The ratio

$$N = \frac{S.A.}{\sqrt[3]{V^2}}.$$

is scale invariant and we will focus on this ratio. To make the numeric integration as accurate as possible, we integrate over small pieces of the surface and then use the symmetries of the surface to compute the surface area. The volume of the lattice can be found by taking the determinant of the matrix that consists of the three period vectors of the lattice. As a check that the region we are integrating over is correct, we check if the surface is genus 3 by using the Gauss-Bonnet theorem.

6.1 The tP Family

The P surface has a cubic lattice and the other members of the tP family have a rectangular prism lattice. We know we can split R^3/Λ with two parallel planes, which have a smaller surface area to volume ratio [Ros05]. The P surface is still an interesting case to study because of the many symmetries it has. Since the P Surface has many symmetries, we only need to compute the surface area of small portions.

First, we should examine the behavior of the surface area-to-volume ratio for small values of $\mathrm{Im}(\tau)$ as seen in Figure 6.1. Figure 6.4 show two P surfaces with smaller values of $\mathrm{Im}(\tau)$. As we get a smaller value of $\mathrm{Im}(\tau)$, the surface starts to look like a pair of planes with catenoid-like necks. Since the volume begins to shrink and the surface area is approximately the surface area of two planes, we get a ratio that tend to infinity. We

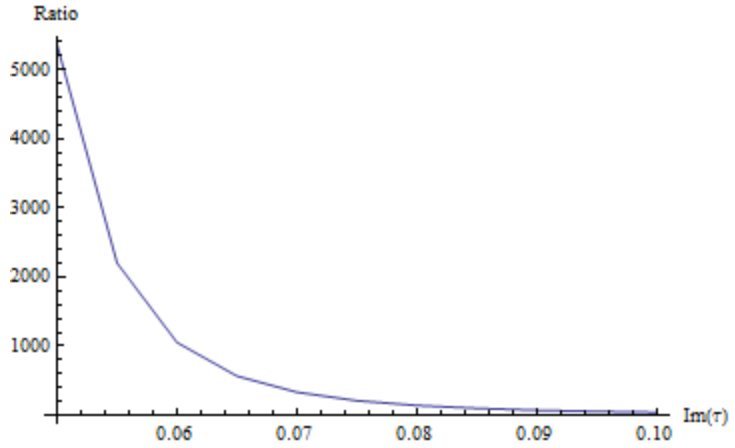

Figure 6.1: This figure shows the surface area-to-volume ratio for tP family with small values of $\mathrm{Im}(\tau)$.

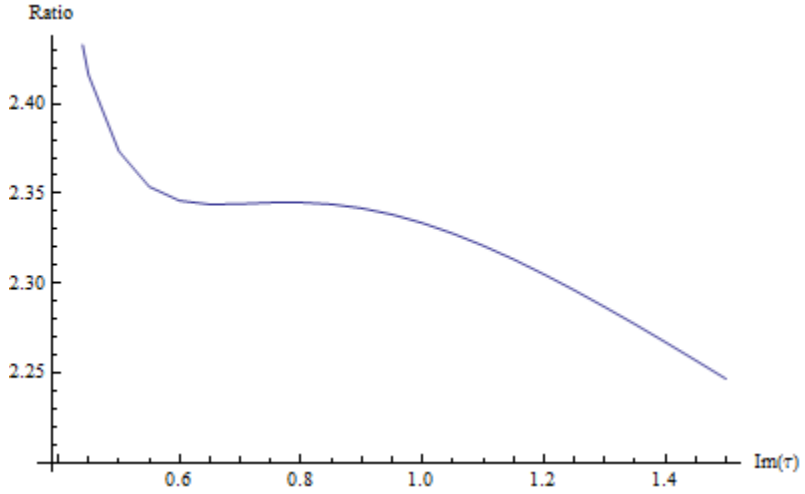

Figure 6.2: This figure shows the surface area-to-volume ratio for tP family with medium values of $\mathrm{Im}(\tau)$.

will not prove this property formally.

Figure 6.2 shows the surface area-to-volume ratio for P surfaces with $0.4 < \mathrm{Im}(\tau) < 1.5$. For these values, we see a smoothing out of values between 0.6 and 0.9. We might suspect that the most symmetric P surface with $\tau \approx 0.7817i$ is a critical point in the graph; however, it does not appear to be the case.

After the smoothing of the graph, we see the surface area-to-volume ratio drop very slowly. We can see this behavior in Figure 6.3 and it appears that the ratio is going to zero (very slowly!). Figure 6.5 shows two P surfaces with a larger values of $\mathrm{Im}(\tau)$. We

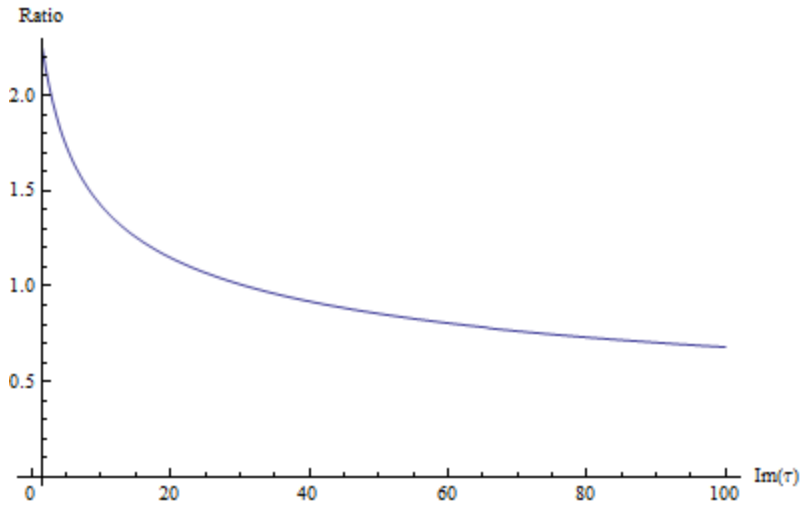

Figure 6.3: This figure shows the surface area-to-volume ratio for tP family with large values of $\mathrm{Im}(\tau)$.

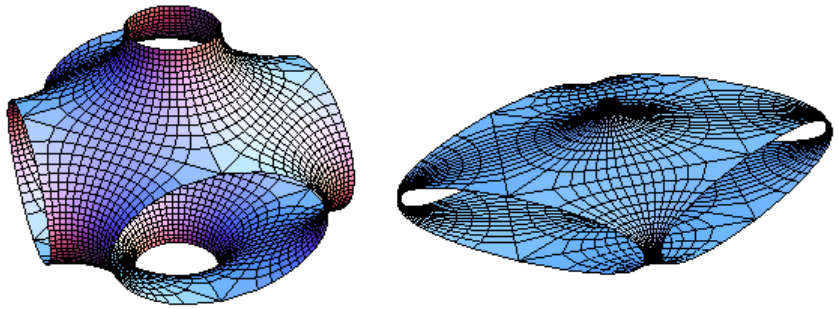

Figure 6.4: Left: The P surface with $\tau = 0.5i$. Right: The P surface with $\tau = 0.25i$

will attempt to explain this behavior, but we will not present a formal proof. The height of the lattice is shrinking, so the volume is approaching zero. We can see the surface begin to widen in the top and bottom holes while the holes on the side are shrinking. The surface is also appears to be pushing up against the walls of the lattice. Thus, the surface area is approaching the area of the sum of the four vertical sides of the rectangular prism lattice. Let v_3 be the norm of the period vector in the z direction and v_1, v_2 be the norms of the period vectors in the x and y direction. Since $v_1 = v_2$, we approximately get

$$\begin{aligned} SAV &\approx \frac{4v_1v_3}{\left(v_1^2v_3\right)^{2/3}} \\ &= \frac{4v_3^{1/3}}{v_1^{1/3}}, \end{aligned}$$

which goes to zero for large values of Imτ.

The most symmetric P surface sits inside a cube and has a surface area-to-volume ration of approximately 2.35. In [Ros03], Ros shows that the a lower bound of the surface area-to-volume ratio for any surface splitting the cube into two invariant regions of equal volume and containing the symmetries of the $P23, P432, Pm\bar{3}, P\bar{4}3m$, or $Pm\bar{3}m$ space group is at least 2.19. This makes the P surface an excellent candidate to solve the isoperimetric problem for surfaces given any of these symmetry restrictions. It is conjectured that the P surface is the surface that solves this isoperimetric problem for these space groups [Ros03].

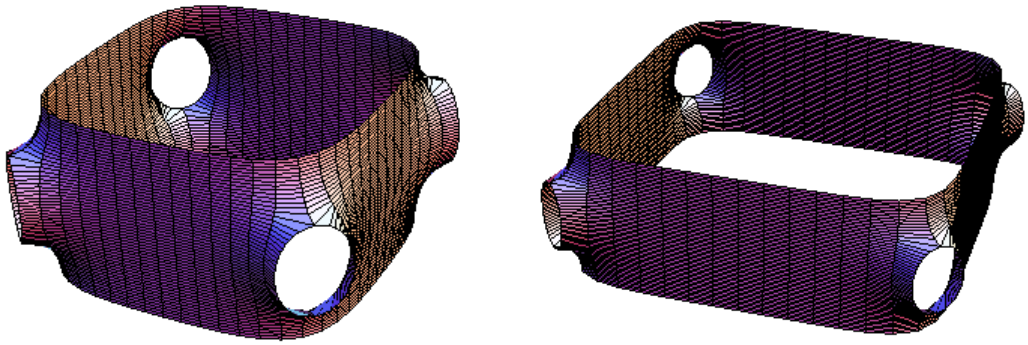

Figure 6.5: Left: The P surface with $\tau = 3i$. Right: The P surface with $\tau = 5i$

6.2 The tD Family

The D surface is not orientable using its the standard lattice. Putting together 8 copies to make a 2 by 2 by 2 block, we can then make a consistent choice of normal. The result of this is that the D surface is no longer genus 3. Instead, we get a genus 9 surface since the Euler characteristic is -16 [Ros03]. Like in the P family, we can use the symmetries of the surface to compute the surface area.

From Figure 6.6 we can examine the limiting behavior of the surface area-to-volume ratio as Im(τ) approaches zero. Like in the P family, the surfaces with smaller values for Im(τ), look like two planes with little helicoid necks. Thus, we once again get a ratio

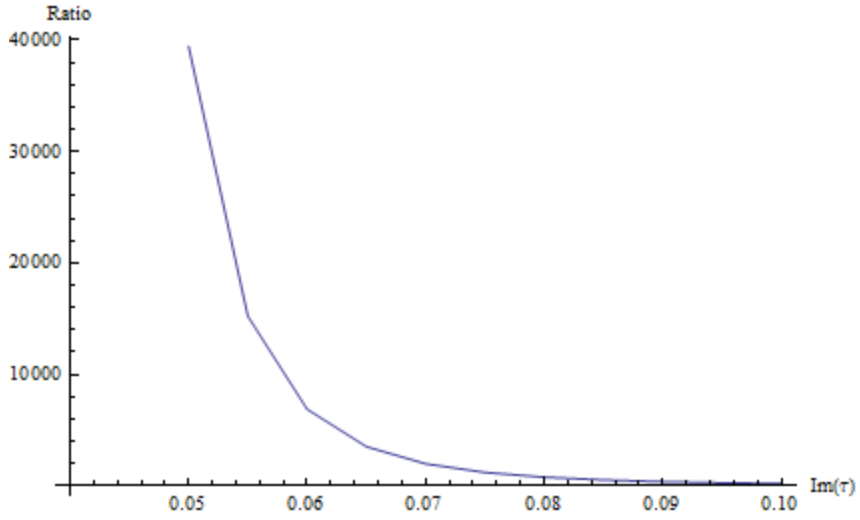

Figure 6.6: This figure shows the surface area-to-volume ratio of tD family where $\mathrm{Im}(\tau)$ is small.

that blows up. We will not present a formal proof of this. Figure 6.9 shows the D surface flatten for some smaller values of $\mathrm{Im}(\tau)$.

Figure 6.7 shows the surface area-to-volume ration for values of τ with $0.1 < \mathrm{Im}(\tau) < 2$. The result are interesting here since we have a local minimum occurring at what may be $\tau \approx 0.7817$, which is the most symmetric D surface. The graph starting to rise, which differs from the P surface graph.

We will attempt to explain the behavior of the graph in Figure 6.8. With larger values of $\mathrm{Im}(\tau)$, we get the height of the lattice increasing as apposed to the P surface lattice which shrinks in height. Once again let v_3 be the norm of the period vector in the z direction and v_1, v_2 be the norms of the period vectors in the x and y direction. Since $v_1 = v_2$, we approximately get

$$\begin{aligned} SAV &\approx \frac{8v_1v_3}{\left(v_1^2v_3\right)^{2/3}} \\ &= \frac{8v_3^{1/3}}{v_1^{1/3}}, \end{aligned}$$

which goes to infinity for large values of $\mathrm{Im}\tau$ since v_1 is decreasing and v_3 is decreasing. We will not present a formal proof of this. We can see the vertical stretching of the

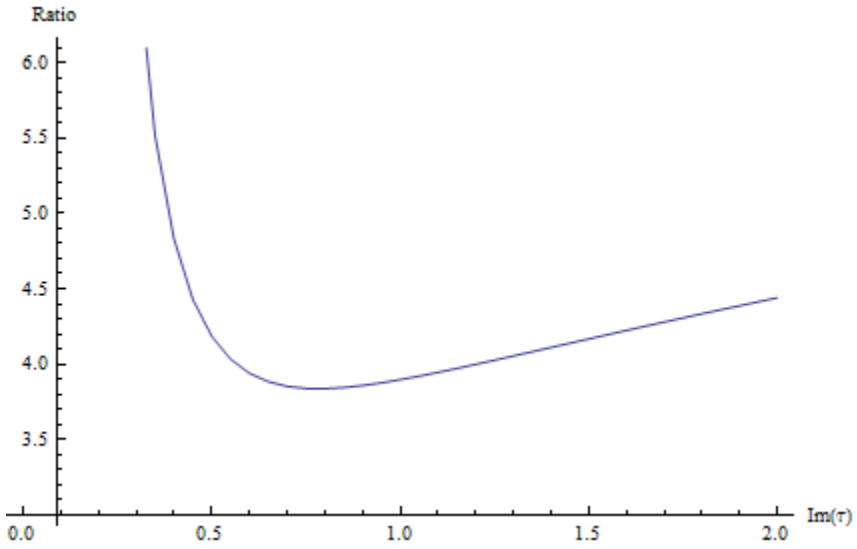

Figure 6.7: This figure shows the surface area-to-volume ratios for tD family members with $0.1 < \mathrm{Im}(\tau) < 2$.

surface for larger values of $\mathrm{Im}(\tau)$ in Figure 6.10.

The most symmetric D surface sits inside a cube has a surface area-to-volume ratio of approximately 3.84. Ros shows that the a lower bound of the surface area-to-volume ratio for any surface splitting the cube into two invariant regions of equal volume and containing the symmetries of the $F4_132, Fd\bar{3}, F\bar{4}3c, Fm\bar{3}c$ or $Fd\bar{3}m$ space group is at least 3.69 [Ros03]. This makes the D surface a good candidate to solve the isoperimetric problem in these situations. In [Ros03], Ros conjectures that the D surface is the solution to the isoperimetric problem for the aforementioned space groups.

6.3 The CLP Family

Like the tD and tP families, the CLP family also has rectangular prism lattices. The CLP surfaces are less symmetric than the P and D, but we can still use symmetries of the surfaces to compute the surface area-to-volume ratios.

Figure 6.11 shows the surface area-to-volume ratios for small values of $\mathrm{Im}(\tau)$. Similar to the tD family, we have a stretching out of the surface in the z direction. This makes the surface area-to-volume ratio grow without bound as $\mathrm{Im}(\tau) \to 0$. Once again, we

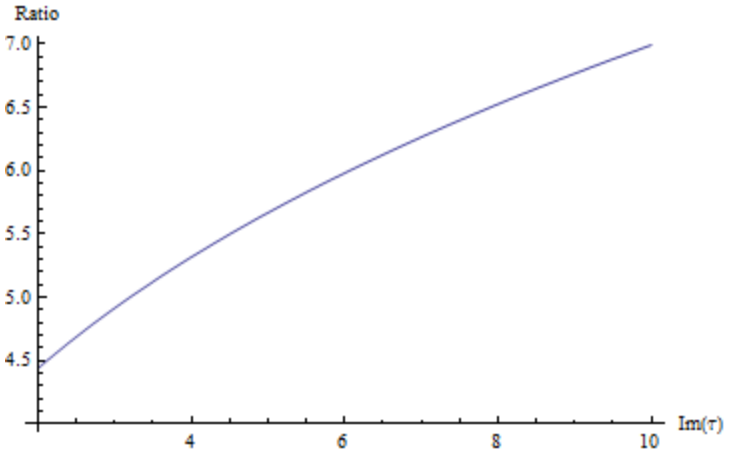

Figure 6.8: This figure shows the surface area-to-volume ratio of tD family where $\mathrm{Im}(\tau)$ is large.

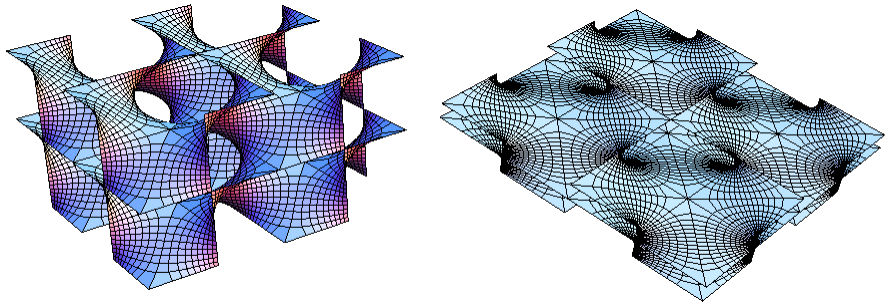

Figure 6.9: Left: The D surface with $\tau = 0.5i$. Right: The D surface with $\tau = 0.25i$

won't show this formally. Figure 6.14 shows a couple of examples of the surface with small values of $\mathrm{Im}(\tau)$.

When we look at the graph in Figure 6.12, we should note that we do not see any critical points. We just get a slow and smooth drop in the ratio. Figure 6.13 shows the behavior for larger values of $\mathrm{Im}(\tau)$. Similar to the tP family, we get the surface smashing up against the lattice wall and the height shrinking. Figure 6.15 shows some pictures of this behavior. Just like in the tP family, we expect the ratio to go to zero.

Finally, we should make a quick note on the isoperimetric problem. Due to less symmetry and larger surface area-to-volume ratios, CLP family members do not appear to be candidates for a solution to the isoperimetric problem.

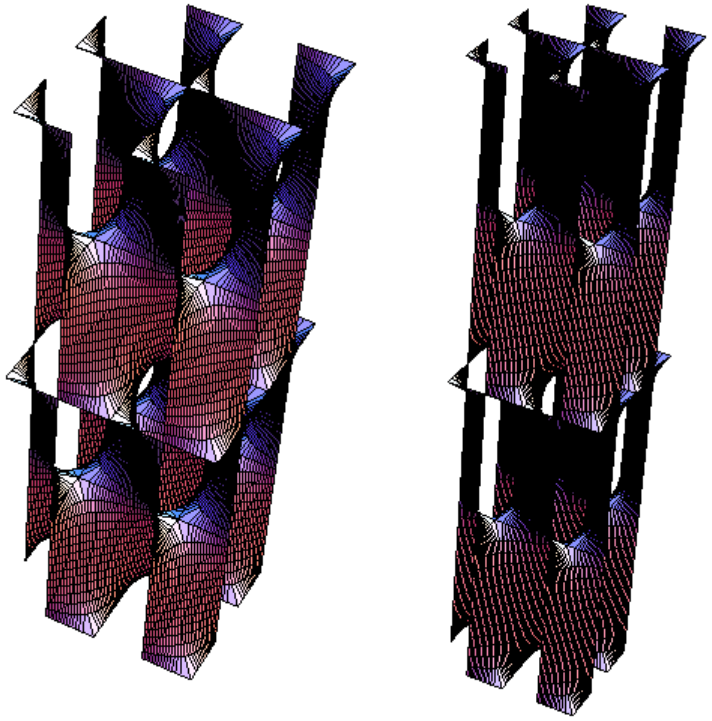

Figure 6.10: Left: The D surface with $\tau = 2i$. Right: The D surface with $\tau = 3i$

6.4 The rH Family

Each rH family members sits in a hexagonal lattice. The surface area-to-volume ratio can be computed using the order 3 rotation and reflectional symmetries. The results are displayed in 6.16.

First, we examine the behavior for small $\mathrm{Im}(\tau)$. Images in Figure 6.17 show two rH family members for smaller values of $\mathrm{Im}(\tau)$. The surface begin approaches a pair of hexagonal planes with catenoid necks as the height shrinks. Let v_1,v_2, and v_3 be the vectors in the z, x, and y directions respectively and let $a_i = |v_i|$. Then for small $\mathrm{Im}(\tau)$, we have

$$\begin{aligned} SAV &\approx \frac{2\,|v_2 \times v_3|}{(|v_2 \times v_3|\, a_1)^{2/3}} \\ &= 2\,|v_2 \times v_3|^{1/3} a_1^{2/3}, \end{aligned}$$

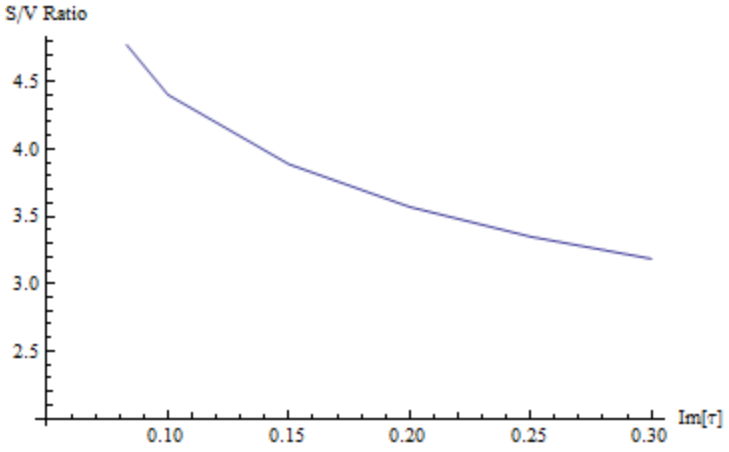

Figure 6.11: This figure shows surface area-to-volume ratios of CLP surfaces with smaller values of $\mathrm{Im}(\tau)$.

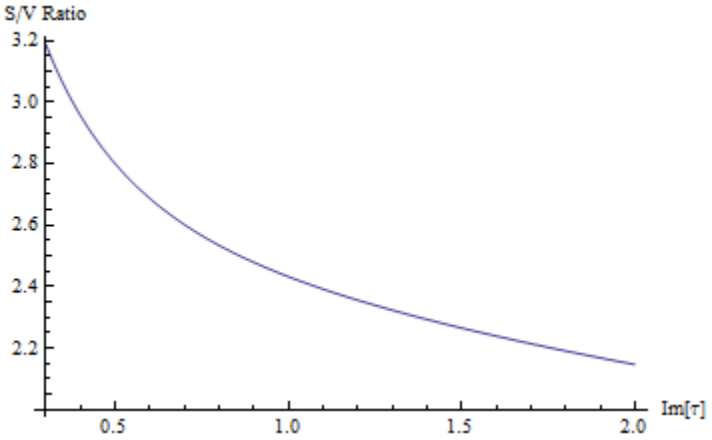

Figure 6.12: This figure shows surface area-to-volume ratios of CLP surfaces with $0.3 < \mathrm{Im}(\tau) < 2$.

which tends to infinitely as $\mathrm{Im}(\tau) \to 0$ since $a_1 \to 0$.

For medium values of $\mathrm{Im}(\tau)$, we see a steady decline in the surface area-to-volume ratio, but we do not see any critical points. For larger values of $\mathrm{Im}(\tau)$, the surface will begin to smash itself into the walls of the lattice as the height shrinks. This behavior can be seen in Figure 6.18. Since $a_2 = a_3$ and $|v_2 \times v_3| = a_2$, then for larger values of $\mathrm{Im}(\tau)$

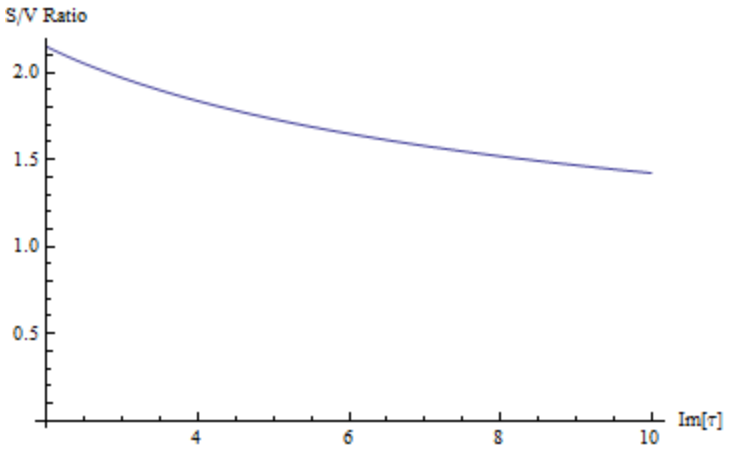

Figure 6.13: This figure shows surface area-to-volume ratios of CLP surfaces with larger values of Imτ.

we have

$$\begin{aligned} SAV &\approx \frac{3a_1a_2}{\left(|v_2 \times v_3|\, a_1\right)^{2/3}} \\ &< \frac{3a_1a_2}{\left(a_1a_2\right)^{2/3}} \\ &= 3\left(a_2a_1\right)^{1/3}, \end{aligned}$$

which tends to 0.

There is less research on the isoperimetric problem for hexagonal lattices. We pose the following question: Is the H surface a good candidate to solve the isoperimetric problem for a hexagonal lattice? The answer is no if we do not put on a symmetry restriction. The graph in Figure 6.19 compares members of the rH family to vertical pairs and horizontal pairs of planes in a hexagonal lattice. Most of the times, the vertical pair of planes are the clear winner. The pair of horizontal planes contain the same space groups as the H surface. We then have that the H surface is not a candidate to solve the isoperimetric problem for smaller values of Imτ. When Im$(\tau) \approx 5.25$, the H surface has a smaller surface area-to-volume ratio than a pair of horizontal planes.

One last thing to note is that for the P and D surfaces, the most symmetric surfaces appear to be critical points for the surface area-to-volume ratio. There is not a "most

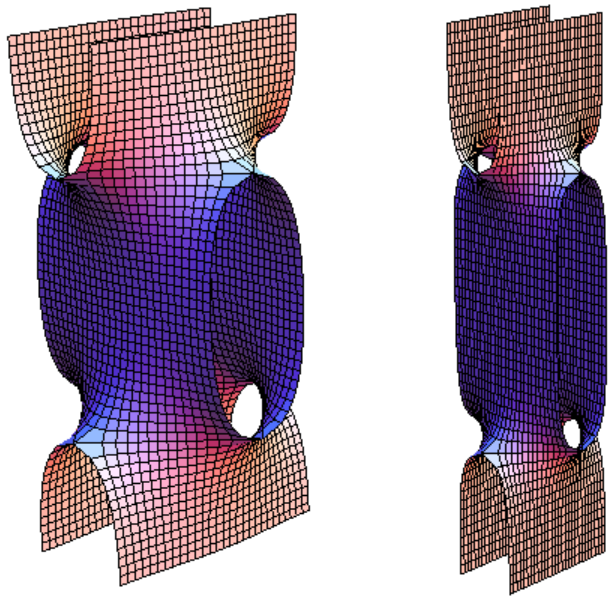

Figure 6.14: Left: The CLP surface with $\tau = 0.5i$. Right: The CLP surface with $\tau = 0.25i$

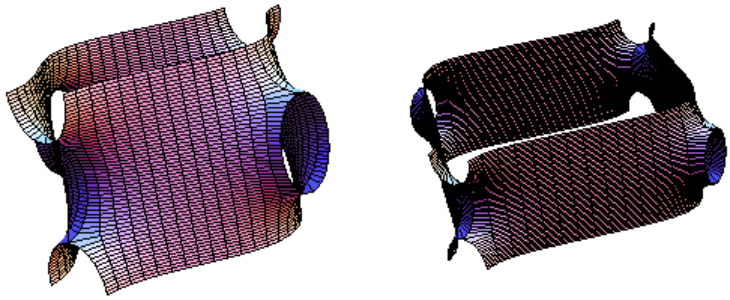

Figure 6.15: Left: The CLP surface with $\tau = 2i$. Right: The CLP surface with $\tau = 4i$

symmetric" H surface and we do not get a critical point for the surface area-to-volume ratio.

6.5 The rPD Family

The rPD family is the first family we look at that has a rhombohedron lattice. We use the order 3 symmetry and reflectional symmetries of the surface to help compute the surface area-to-volume ratio.

Figure 6.21 shows the surface area-to-volume ratio for smaller values of $\mathrm{Im}(\tau)$. We see ratio blowing up as $\mathrm{Im}(\tau)$ approaches zero. Figure 6.22 shows two surfaces with smaller

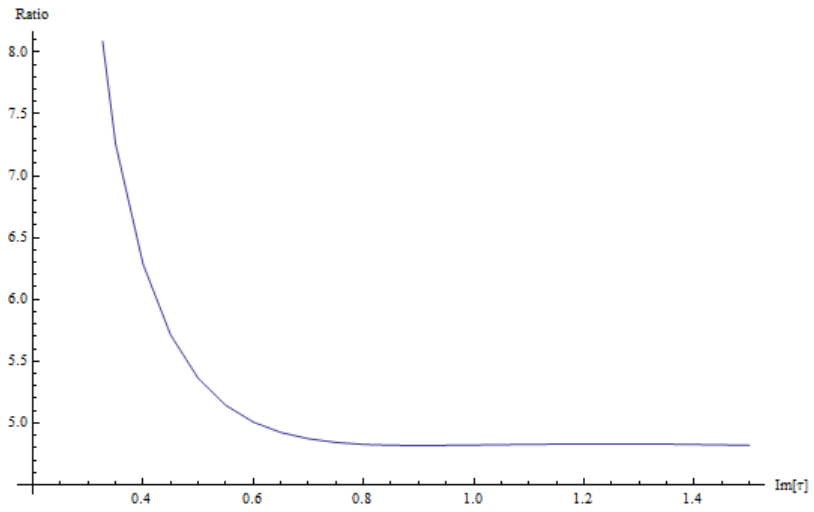

Figure 6.16: This figure shows surface area-to-volume ratios of H surfaces as Imτ increases.

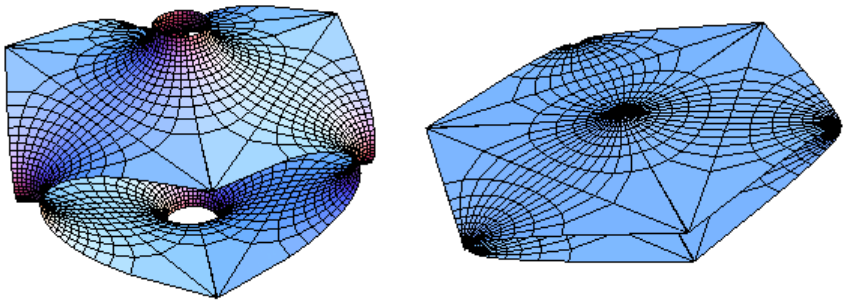

Figure 6.17: Left: The H surface with $\tau = .5i$. Right: The H surface with $\tau = .25i$

values for Im(τ). We expect the surface ratio to blow up because we can see the surface begin to pancake as the lattice shrinks.

Figure 6.23 shows the surface area-to-volume ratio for PD surfaces with $0.4 <$ Im(τ) < 3. We can point out two points of interest. At around $\tau = 0.6i$ we see a local maximum point and we see a local minimum point at around $\tau = 1.5i$.

Figure 6.24 shows the surface area-to-volume ratio for larger values of Im(τ). We see the ratio blowing up as Im(τ) goes to infinity. Figure 6.25 shows two surfaces with larger values for Im(τ). We expect the surface ratio to blow once again because we get the similar pancaking behavior as the lattice shrinks.

Now we would like look at if the rPD family has any members that solve the isoperi-

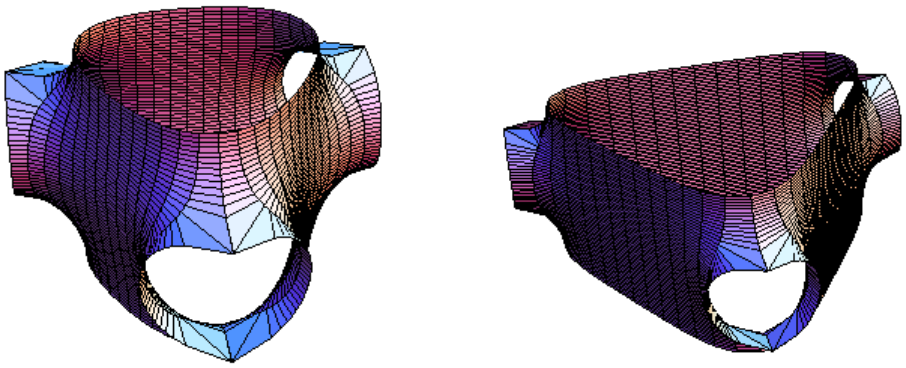

Figure 6.18: Left: The H surface with $\tau = 2i$. Right: The H surface with $\tau = 4i$

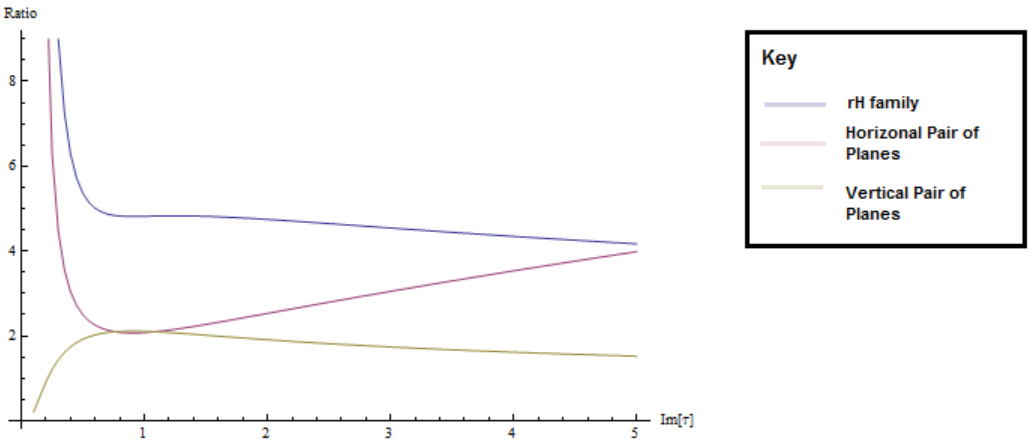

Figure 6.19: Comparing the surface area-to-volume ratios of the rH family to pairs of vertical and horizontal planes.

metric problem. In Figure 6.26 and Figure 6.27 we compare the surface area-to-volume ratio of members of the rPD family to pairs of rhombus shaped planes parallel to on of the faces of the lattice. We do not see the surface being a solution for any value of τ. The surfaces do contain symmetries that the planes do no have and therefore may be candidates when the isoperimetric problem calls for theses symmetries.

6.6 The Gyroid/Lidinoid

The gyroid and Lidinoid share a one parameter are family [Wey06]; however, the actual values for τ are not known at the moment. We like to present some numeric data to argue that a particular sequence of τ gives us this family. In the graphs, the

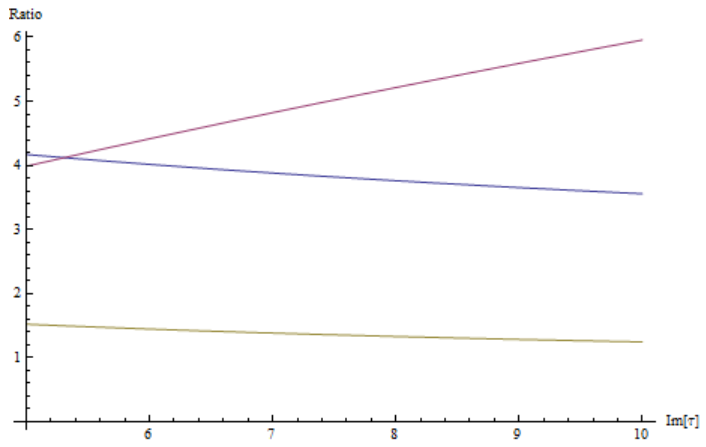

Figure 6.20: Comparing the surface area-to-volume ratios of the rH family to pairs of vertical and horizontal planes for larger values of Im(τ).

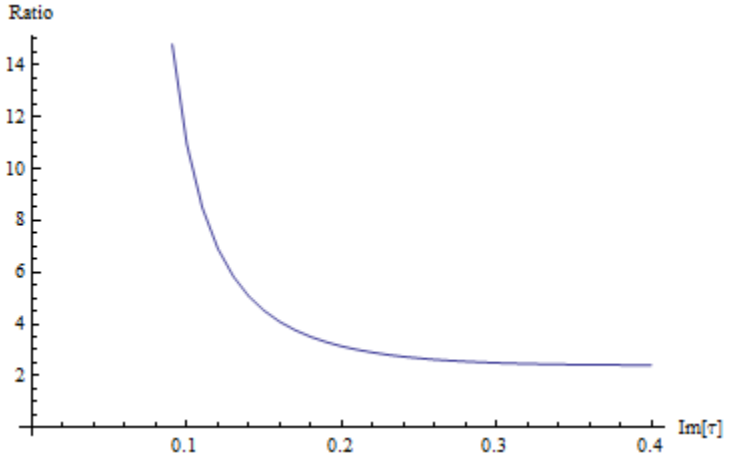

Figure 6.21: This figure shows surface area-to-volume ratios of PD surfaces with smaller values of Im(τ).

horizontal axis will represent the values in the array. Surfaces parameterized by τ on the left of the Lidinoid are part of a Lidinoid family (the Lidinoid is in the $50th$ position in the array). The gyroid is in the $100th$ position of the array. The values between the gyroid and Lidinoid are the possible family between the two surfaces. The surfaces to the right of the gyroid are members of the gyroid family. In this section we also look at the surface area-to-volume ratios in this potential family. We will be calling this family the rGL family. Each member has a rhombohedron shaped lattice and admit an order3 symmetry.

We can see a couple of interesting things in Figure 6.28. First, we see a local maximum

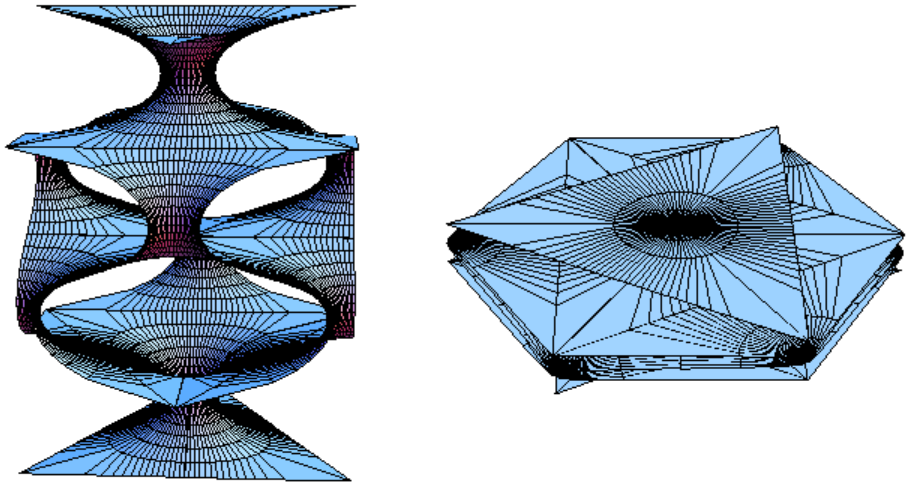

Figure 6.22: Left: The PD surface with $\tau = .25i$. Right: The PD surface with $\tau = .1i$

of the graph near or at the value of the gyroid. We can also see that the graph is smooth, which may be evidence that this is the correct sequence of τ that give us a gyroid-Lidinoid family.

Figure 6.29 compare different members of the family to a pair of planes parallel to the one pair of faces in the rhombohedron lattice. When we look at the surface area-to-volume ratios to surfaces right of the gyroid, we begin to surfaces that beat the pair of planes. These surface have potential to be solutions in the case we require more symmetry since the pair of planes dose not have an order 3 rotational symmetry.

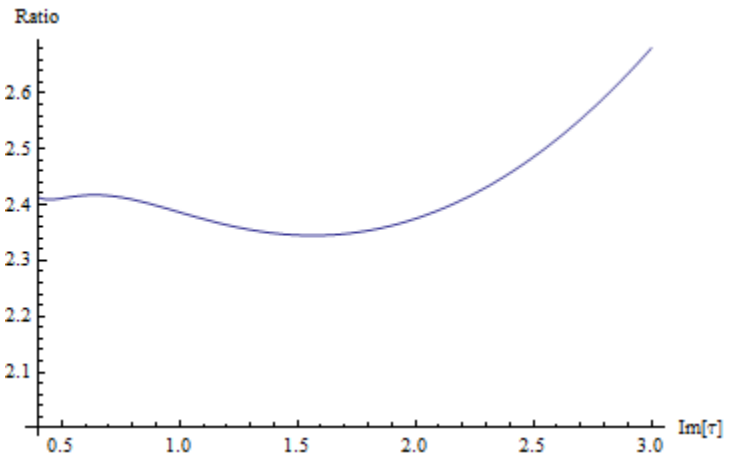

Figure 6.23: This figure shows surface area-to-volume ratios of PD surfaces with $0.4 < \mathrm{Im}(\tau) < 3$.

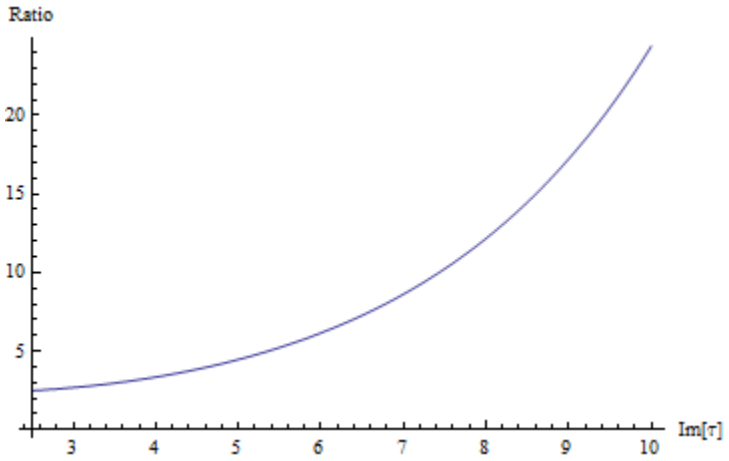

Figure 6.24: This figure shows surface area-to-volume ratios of PD surface for larger values of $\mathrm{Im}\tau$.

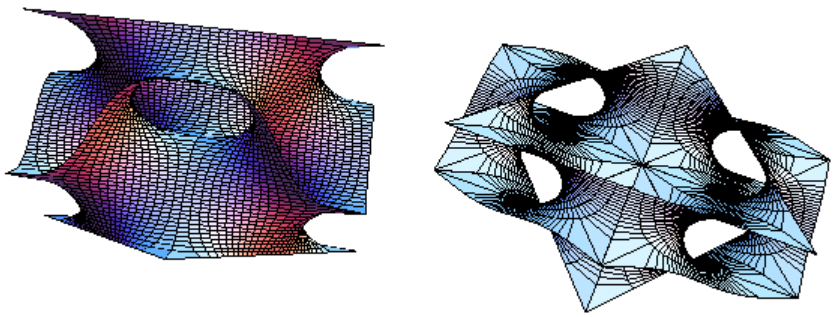

Figure 6.25: Left: The PD surface with $\tau = 2i$. Right: The PD surface with $\tau = 4i$

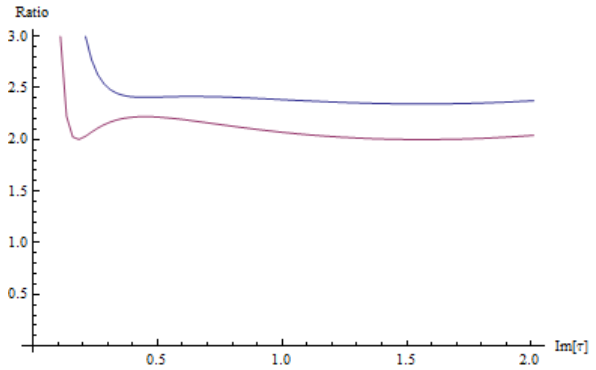

Figure 6.26: Comparing the surface area-to-volume ratios of the rPD family (purple) to pairs of horizontal planes (red).

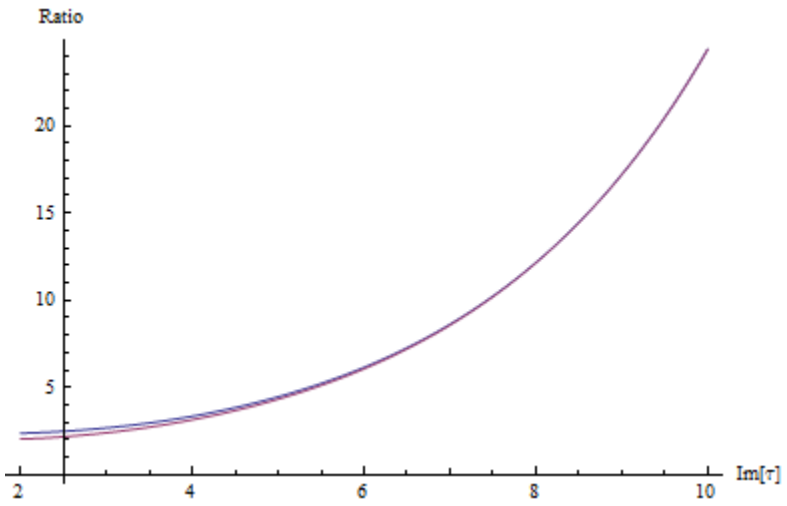

Figure 6.27: Comparing the surface area-to-volume ratios of the rPD family to pairs of horizontal planes for larger values of $\mathrm{Im}(\tau)$.

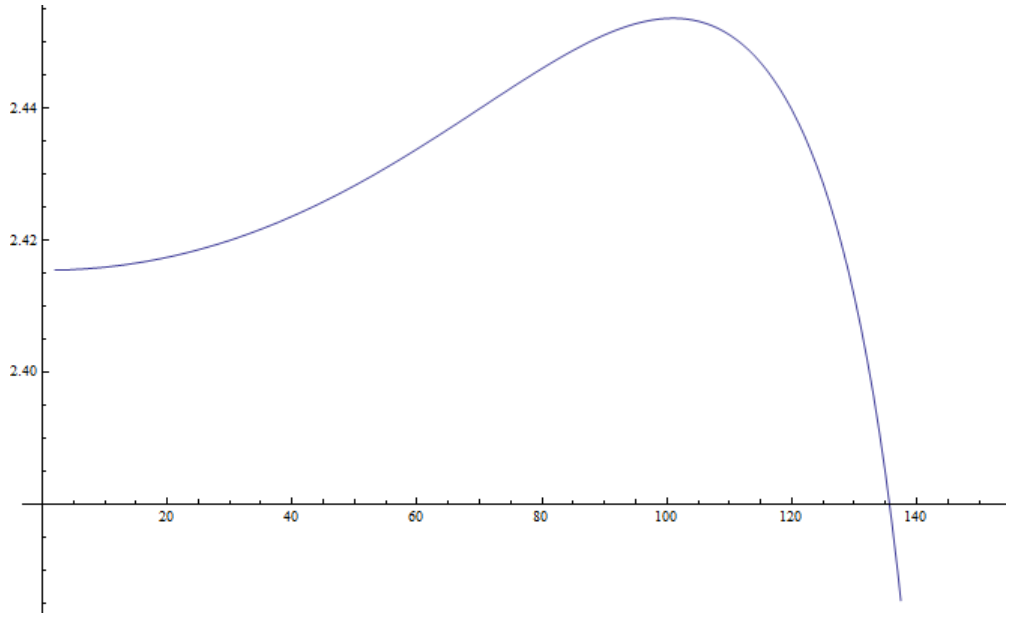

Figure 6.28: Looking at the surface area-to-volume ratio for different members of the rGL family.

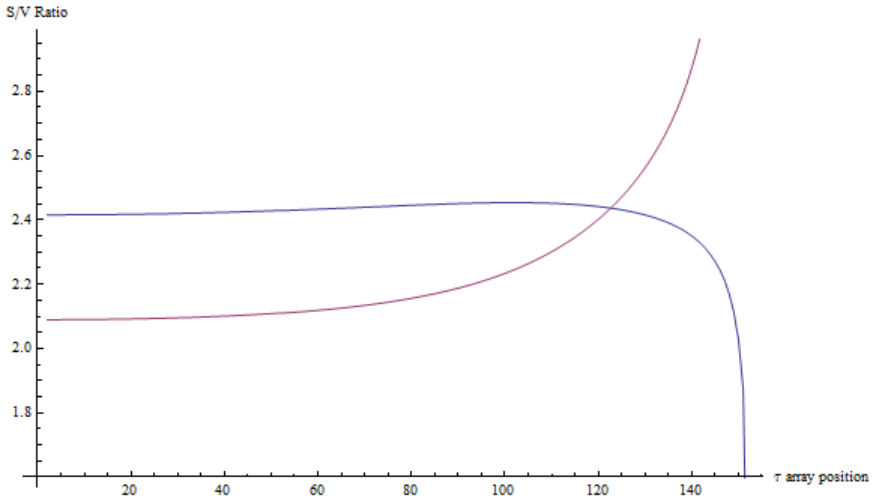

Figure 6.29: Comparing the surface area-to-volume ratios of the rGL family to pairs of planes for values of τ.

CHAPTER 7

CONCLUSION

In this thesis, we have shown that certain genus g triply periodic minimal surfaces split their lattices into two spaces of equal volumes. With this problem we were able to search for possible candidates to solve the isoperimetric problem for different lattices. While most surface were not solutions to the problem, we did see some surfaces that may solve the problem when we add a symmetry restriction.

This analysis leads us to many open questions. The most obvious question to ask, what surface solve the isoperimetric problem? If we begin to understand surfaces that split $\mathbb{R}^3/\Lambda$, we may be able to understand more complicated situations as well.

REFERENCES

[Car63] Henri Cartan. *Elementary theory of analytic functions of one or several complex variables*. Hermann, Paris, first edition, 1963.

[FK92] H. M. Farkas and I. Kra. *Riemann surfaces*, volume 71 of *Graduate Texts in Mathematics*. Springer-Verlag, New York, second edition, 1992.

[GBW96] Karsten Große-Brauckmann and Meinhard Wohlgemuth. The gyroid is embedded and has constant mean curvature companions. *Calc. Var. Partial Differential Equations*, 4(6):499–523, 1996.

[LL90] Sven Lidin and Stefan Larsson. Bonnet transformation of infinite periodic minimal surfaces with hexagonal symmetry. *J. Chem. Soc. Faraday Trans.*, 86(5):769–775, 1990.

[Mas91] William S. Massey. *A Basic Course in Algebraic Topology*, volume 127 of *Graduate Texts in Mathematics*. Springer, New York, first edition, 1991.

[Mee75] William H. Meeks, III. *The Geometry and the Conformal Structure of Triply Periodic Minimal Surfaces in* $\mathbb{R}^3$. PhD thesis, University of California, Berkeley, 1975.

[Mee81] William H. Meeks, III. The theory of triply periodic minimal surfaces. *Topology*, 20:389–410, 1981.

[Mee90] William H. Meeks, III. The theory of triply periodic minimal surfaces. *Indiana Univ. Math. J.*, 39(3):877–936, 1990.

[Ros03] Antonio Ros. Isoperimetric inequalities in crystallography. *Journal of the American Mathematical Society*, 317(2):373–388, 2003.

[Ros05] Antonio Ros. The isoperimetric problem, proceedings of the clay mathematical institute msri summer school on minimal surfaces, global theory of minimal surfaces. *Clay Math. Proc., 2, Amer. Math. Soc*, pages 175–209, 2005.

[San94] Donald E. Sands. *Introduction to Crystallography*. Dover Publications, Paris, reprint edition, 1994.

[Sch90] H.A. Schwarz. *Gesammelte Mathematische Abhandlungen, 2 Bände*. Springer, Berlin, 1890.

[Sch70] Alan H. Schoen. Infinite periodic minimal surfaces without self-intersections. *NASA Technical Note TN D-5541*, 1970.

[Tra08] Martin Traizet. On the genus of triply periodic minimal surfaces. *J. Diff. Geom.*, 79(2):243–275, 2008.

[Web04] Matthias Weber. Notes on minimal surfaces. Lecture notes for a course at Indiana University, April 2004.

[Wey06] Adam G. Weyhaupt. *New Families of Embedded Minimal Surfaces of Genus Three in Euclidean Space*. PhD thesis, Indiana University, Bloomington, Indiana, August 2006.